Control of dental derived stem cell and its application for improvement of bone regeneration

Hyunmin Choi

The Graduate School

Yonsei University

Department of Dentistry

Control of dental derived stem cell and its application for improvement of bone regeneration

A Dissertation

Submitted to the Department of Dentistry

and The Graduate School of Yonsei University

in partial fulfillment of the

requirements for the degree of

Doctor of Philosophy in Dental Science

Hyunmin Choi

December 2017

This certifies that the dissertation of

Hyunmin Choi is approved.

_____
Thesis Supervisor: Young-Bum Park

_____
June-Sung Shim

_____
Hong-Seok Moon

_____
Hyung-Jun Kim

_____
Seung-Han Oh

The Graduate School
Yonsei University
December 2017

TABLE OF CONTENTS

LIST OF FIGURES

CHAPTER 1

Generation of dental-derived induced pluripotent stem cells and control of dental-derived induced pluripotent stem cells through modified surfaces of Ti disc for dental application

LIST OF TABLES

LIST OF FIGURES

CHAPTER 2

In vivo study for clinical application of dental stem cell therapy incorporated with dental implant

LIST OF TABLES

Chapter 1

Generation of dental-derived induced pluripotent stem cells and Control of dental-derived induced pluripotent stem cells through modified surfaces of Ti disc for dental application

ABSTRACT

Generation of dental-derived induced pluripotent stem cells and Control of dental-derived induced pluripotent stem cells through modified surfaces of Ti discs for dental application

Hyunmin Choi

Department of Dentistry
The Graduate School, Yonsei University

(Directed by Professor Young-Bum Park)

Purpose The aim of this study is to investigate the behavior of iPSc derived from dental stem cells in terms of initial adhesion, differentiation potential on differently surface-treated titanium disc.

Methods iPSc derived from human gingival fibroblasts (hGFs) were established using 4-reprogramming factors transduction with Sendai virus. The hGF-iPSc established in this study exhibited the morphology and growth properties similar to human embryonic stem (ES) cells and expressed pluripotency makers. Alkaline Phosphatase (AP) staining, Embryoid Body (EB) formation & *in vitro* differentiation and karyotyping further confirmed pluripotency of hGF-iPSc. Then, hGF-iPSc were cultured on machined- and

Sandblasted and acid etched (SLA)-treated titanium discs with osteogenic induction medium and their morphological as well as quantitative changes according to different surface types were investigated by using Alizarin Red S staining, Scanning electron microscopy (SEM), Flow cytometry and RT-PCR.

Results Time-dependent and surface-dependent morphological changes as well as quantitative change in osteogenic differentiation of hGF-iPSc were identified and osteogenic gene expression of hGF-iPSc cultured on SLA-treated titanium disc found to be greater than machined titanium disc, suggesting the fate of hGF-iPSc may be determined by the characteristics of surface to which hGF-iPSc first adhere.

Conclusion iPSc derived from dental stem cell can be one of the most promising and practical cell sources for personalized regenerative dentistry and their morphological change as well as quantitative change in osteogenic differentiation according to different surface types of implants may be further utilized for future clinical application incorporated with dental implant.

Keyword : *induced pluripotent stem cells derived from dental stem cells, characterization, titanium disc, rough surface, osteogenesis*

Ⅰ. INTRODUCTION

Edentulism remains as a major challenge for contemporary dentistry and continuous progress attempting to improve the osseointegration is still being made in order to achieve high success rate in implant therapy. As a consequence, there have been many *in vitro* studies to better understand the mechanisms underlying cell to implant interactions including cell adhesion, proliferation, differentiation and matrix deposition.(1-3)

The conditions of limited bone healing potential due to poor bone quality and quantity may lead to increased implant failure rates and for this reason, bone augmentation is required in implant placement site when insufficient bone volume is present. Autologous bone graft has been well-documented to be one of the most reliable and effective surgical approaches and is also accepted as the gold standard treatment modality for patient with insufficient bone volume.(4) However, due to considerably high morbidity including pain, infection and loss of function, alternative tissue engineering technique based on autologous cell transplantation has been emerged to find new ways to improve the kinetics of osseointegration, ultimately increasing total bone volume around implant site. (5)

Bone marrow-derived mesenchymal stem cells (BMMSCs) have long received much attention as primary cell sources for autologous cell transplantation because of their self-renewal properties and ability to differentiate into many cellular lineages, including osteocytes, adipocytes, and chondrocytes.(6, 7) Also, BMMSCs have been reported to

exhibit potent immunomodulatory capacity, (8, 9) which places BMMSCs the most suitable tools for the treatment of bone defect-related disease. (10, 11) Nevertheless, BMMSC's self-renewal and proliferative ability decreases due to aging and diseases such as osteoporosis and arthritis, making it very difficult to obtain adequate cell numbers required for implantation. Moreover, current methods for obtaining BMMSCs from patients are surgically invasive, leading to substantial morbidity of donor site including pain, infection and loss of function. (12) Therefore, it is of paramount importance that alternative source of BMMSCs which can overcome the aforementioned limitation of BMMSCs before they can be used as a standard treatment modality for cell-based bone tissue engineering.

The recent development in induced pluripotent stem cell (iPSc) offers many advantages over traditional MSC including easiness to generate from almost any tissue in the body as well as unlimited growth capacity which circumvents the disadvantage of BMMSCs, and many promising in *in vitro, in vivo* results for application of using iPSc in regenerative medicine have been documented.(13-16) In particular, iPSc derived from dental stem cell including human gingival fibroblast (hGF) attained a special interest due to safety and easiness obtained by surgery, and relatively higher efficiency in reprogramming.(17, 18) However, to date, there have been very few studies reported regarding the behavior of iPSc derived from dental stem cells depending on different surface characteristics of implants. Therefore, the aim of this study is to investigate the behavior of iPSc derived from dental stem cells in terms of initial adhesion, differentiation potential on differently surface-treated titanium disc.

Ⅱ. MATERIALS AND METHODS

Primary culture of hGF

Approval from the Institutional Research Ethics Committee of the Yonsei University College of Dentistry was obtained. (IRB No. 2-2014-0012). After obtaining informed consent, hGF were taken from healthy volunteers, female (Donor 1) aged 16 years old, undergoing orthodontic treatment at Yonsei University Dental Hospital. Gingival tissue was collected and prepared as previous reported (19). Briefly, collected tissues were washed twice with 70% of ethanol then washed again with phosphate buffered saline (PBS; Invitrogen, Waltham, MA, USA) and digested with collagenase I (2 mg/mL; Sigma Aldrich, St. Louis, MO, USA) and dispase II (4 mg/mL; Roche Diagnostics, Indianapolis, IN, USA) for 2 hours at 37°C incubation and the dissociated cells were then seeded on 10-cm tissue culture dishes in a standard cell culture medium, consisting of Dulbecco's modified Eagle's medium (DMEM; Invitrogen) containing 10 % fetal bovine serum (FBS; Invitrogen) and antibiotics (50 U/ml penicillin G and 50 μg/ml streptomycin (P/S); Invitrogen). These cells were incubated at 37 °C in a humidified atmosphere containing 5 % CO_2 for 10 days. *In vitro*-expanded hGFs were maintained under the same culture conditions and hGF at passage 5 was used in this study

.

Induction of iPSc

Induction of iPSc from primary hGFs (passage 5) via transduction of four factors was performed using a CytoTune™ Sendai Reprogramming system (Invitrogen) according to the manufactures' protocol. Using this protocol, twenty-four hours before transduction, hGFs were seeded at 5×10^5 cells per 6-well dishes in standard medium. For the transduction, hGFs were incubated in Sendai viruses-containing medium for 24 h, followed by incubation with standard medium, which was replaced every day. Seven days later, the cells were harvested and 5×10^4 cells were placed on mitomycin-C (Sigma-Aldrich) inactivated mouse embryonic fibroblast (MEF; CEFO bio inc, Seoul, Korea) feeder cells in a 10-cm dish in iPSc culture medium, which consisted of DMEM/F12 (Invitrogen), 20% serum replacement (SR, Invitrogen), 2 mM L-glutamine (Sigma-Aldrich), 1% nonessential amino acids (Invitrogen), 100μM 2-mercaptoethanol (Sigma-Aldrich), 1% P/S and 4ng/ml human basic fibroblast growth factor (bFGF, R&D systems, Minneapolis, MN, Canada). The medium was changed every day, and the cells were monitored daily for any morphological changes. At 30 days after transduction, colonies showing embryonic stem (ES) cell-like morphology, including a round shape, large nucleoli and scant cytoplasm, were mechanically selected for establishing iPSc cultures.

Alkaline phosphatase staining and immunocytochemistry

Alkaline phosphate (AP) staining and immunocytochemical procedure was carried out as described previously(20). For immunocytochemistry, following isotype-specific primary

antibodies were used: OCT4 (1:100 dilution; Santa Cruz Biotechnology, Santa Cruz, CA, USA), NANOG (1:200 dilution; Millipore, San Diego, CA USA), SSEA4 (1:100 dilution; Millipore), SOX2 (1:100 dilution; Millipore), TRA-1-60 (1:200 dilution; Millipore) and TRA-1-81(1:100 dilution; Millipore). For the confirmation of 3-germ layer differentiation, β-tublinIII (ectoderm, 1:100 dilution; Millipore), brachyury (mesoderm, 1:100 dilution; Millipore) and alpha-feto protein (AFP, endoderm, 1:100 dilution; Millipore) were also stained. The secondary antibodies; rhodamine or alexa fluor 488 conjugated rabbit IgG, anti-mouse IgG or anti-mouse IgM (Molecular probe; Invitrogen) were used for antibody localization. Cell nuclei were counterstained with 4′-6-diamidino-2-phenylindole (DAPI) (10 μg/mL; Sigma-Aldrich).

Karyotyping

Standard G-banding chromosome analysis was performed at GenDix cytogenetics laboratory inc (Seoul, Korea) with hGF-iPSc collected at passage 15.

***in vitro* differentiation of iPSc derived from dental stem cell**

Embryoid body (EB) formation followed by *in vitro* differentiation was analyzed in accordance with the protocol of Ohnuki et al.(20) . In brief, iPSc were dissociated with 4 mg/mL of Dispase I and transferred to 60mm petri-dishes in iPSc medium without bFGF. After 8 days in suspension culture, once hGF-iPSc formed ball-shaped structure, hGF-iPScs were transferred to 0.1% gelatin-coated plates to induce further differentiation for

5 days. Differentiated markers such as AFP for endoderm, brachyury for mesoderm, and β-tubulin III for ectoderm were analyzed by immunocytochemistry.

For osteogenic differentiation, hGF-iPSc were cultured in osteogenic medium containing 10mM β-Glycerophosphate (β-GP, Sigma-Aldrich), 10μM dexamethasone and 50μM ascorbic acid for 21 days and fixed with 2% paraformaldehyde. Alizarin red S (Abcam, Cambridge, MA, USA) and Von Kossa (Abcam) staining were performed to evaluate osteogenic differentiation of hGF-iPSc.

Direct differentiation on differently surface-treated titanium disc

hGF-iPSc were cultured at 1 x 10^5 cells on machined-and SLA-treated titanium disc with osteogenic media containing β-GP, dexamethasone, ascorbic acid and their time-dependent and surface-dependent changes were investigated for 28 days using Alizarin Red S staining, Scanning electron microscopy (SEM) and RT-PCR.

Alizarin Red S Staining Quantification Assay Detection and quantification of mineralization

Measurement of alizarin red S (ARS) were performed by Osteogenesis assay kit (Millipore) according to manufacturer's guideline. Briefly, both undifferentiated cells and osteogenic differentiated iPS cells on titanium discs were washed with PBS and fixed in 10% (v/v) para-formaldehyde (Sigma–Aldrich) at room temperature for 15 min. The titanium discs were washed twice with excess dH_2O prior to addition of 1 mL of 40 mM ARS (pH 4.1) solution per well. The plates were incubated at room temperature for

20 min with gentle shaking and washed out unincorporated dye. For quantification of staining, 10% (v/v) acetic acid was added to each well, and the plate was incubated at room temperature for 30 min with shaking. The osteogenic differentiated hGF-iPSc, now loosely attached to the plate, was scraped from the plate with a cell scraper (SPL), followed by transferring to a 1.5-mL micro centrifuge tube with 10% (v/v) acetic acid and heating to 85 °C for 10 min, and transferring to ice for 5 min. The slurry was then centrifuged at 20,000g for 15 min and 500 L of the supernatant was removed. Then, 200 L of 10% (v/v) ammonium hydroxide was added to neutralize the acid. To make up ARS standards, each 2, 1 mM, 500, 250, 125 and 62.5 μM of ARS solution were prepared. The supernatant and standards were read in triplicate at 405 nm in 96-well format using opaque-walled, transparent-bottomed plates.

SEM analysis

hGF-iPSc were cultured at 1 x 10^5 cells on machined-and SLA-treated titanium disc with osteogenic media containing β-GP, dexamethasone, ascorbic acid and their time-dependent and surface-dependent morphological changes were investigated for 28 days using SEM (Hitachi, S-800, Japan)

Flow cytometric analysis

Cells were detached from the culture dish using Triple express solution (Invitrogen), centrifuged, rinsed and re-suspended in PBS at a concentration of 1 x 10^5 cells/mL. Re-suspended cells were incubated with 5 μL of fluorescein isothiocyanate-labeled anti-rat

human osteocalcin (BD Pharmingen, CA, USA) in the dark at 4 °C for 30 min. After being washed twice with PBS, cytometric analysis was performed using a flow cytometer (BD FACS Verse).

Quantitative RT-PCR analysis

Total RNA was isolated using TRIzoL® reagent (Invitrogen). The quality of the RNA was evaluated using spectrophotometry and denaturing agarose gel electrophoresis. cDNA was synthesized from 1 μg of purified total RNA using a PrimeScript RT reagent kit (Invitrogen), according to the manufacturer's instructions. The used primer sequences were described in Table 1. Quantitative RT-PCR analysis was performed with SYBR green real-time PCR master mix (Thermo Fisher scientific) in a 7500 Real-Time PCR System (Thermo Fisher scientific). The PCR conditions were 95°C for 30 s, 40 cycles of denaturation at 95°C for 5 s and annealing and extension at 60°C for 15 s, followed by dissociation and a standard denature action curve.

Statistical Analysis

Mean values represent the mean ± standard deviation (SD). Statistical analyses were performed using ANOVA, followed by Bonferroni correction for multiple comparisons, using the SPSS program (SPSS 13.0). A value of $p < 0.05$ was considered statistically significant.

Gene name	Gene ID	sequences	Amplicon length (bp)
Human GAPDH F	M33197.1	cgaccactttgtcaagctca	203
Human GAPDH R		aggggagattcagtgtggtg	
Human AFP F	NM_001134	agcttggtggtggatgaaac	200
Human AFP R		tccaacaggcctgagaaatc	
Human b-tublin F	NM_006086.3	cgcatcatgaacaccttcag	207
Human b-tublin R		cgataccaggtggttgaggt	
Human IBSP F	NM_004967.3	cgccaatgaatacgacaatg	196
Human IBSP R		gatgcaaagccagaatggat	
Human brachyury F	NM_003181.3	acgccatgtactccttcctg	204
Human brachyury R		tgagcttgttggtgagcttg	
Human COL1A1 F	NM_000088.3	ggcccagaagaactggtaca	200
Human COL1A1 R		cgctgttcttgcagtggtag	
Human BGLAP F	NM_199173.4	ggcagcgaggtagtgaagag	194
Human BGLAP R		agcagagcgacaccctagac	
Human RUNX2 F	NM_001015051.3	agtgccagctgcatcctatt	201
Human RUNX2 R		tgcttgaatttttcccaagg	

Table 1. RT-PCR primer information

Ⅲ. Results

iPSc derivation and characterization

Before transduction of the OCT3/4, SOX2, KLF4, and c-MYC, hGF displayed typical fibroblast spindle-like morphology and developed cluster-like appearance after day 2. The ES cell-like morphology became more outstanding 14 days post transduction. (Fig1A). Also, after suspension culture without inclusion of bFGF in 8 days, round-shaped EB structures were identified with the prominent germ layer formed on peri-radicular region. (Fig1B)

For characterization, we first analyzed undifferentiated status of hGF-iPSc using alkaline phosphate (AP) staining. Strong AP activity was observed (Fig1B) and Standard Q-band chromosome analysis also exhibited the normal karyotyping of hGF-iPSc compared to hGF, showing the iPScs we produced were cytogenetically stable. (Fig1C) Pluripotent stem cell markers, OCT4, NANOG, SOX2, SSEA4, TRA-1-60 and TRA-1-80 were identified by immunocytochemical analysis in all colonies collected for the analysis. (Fig1D)

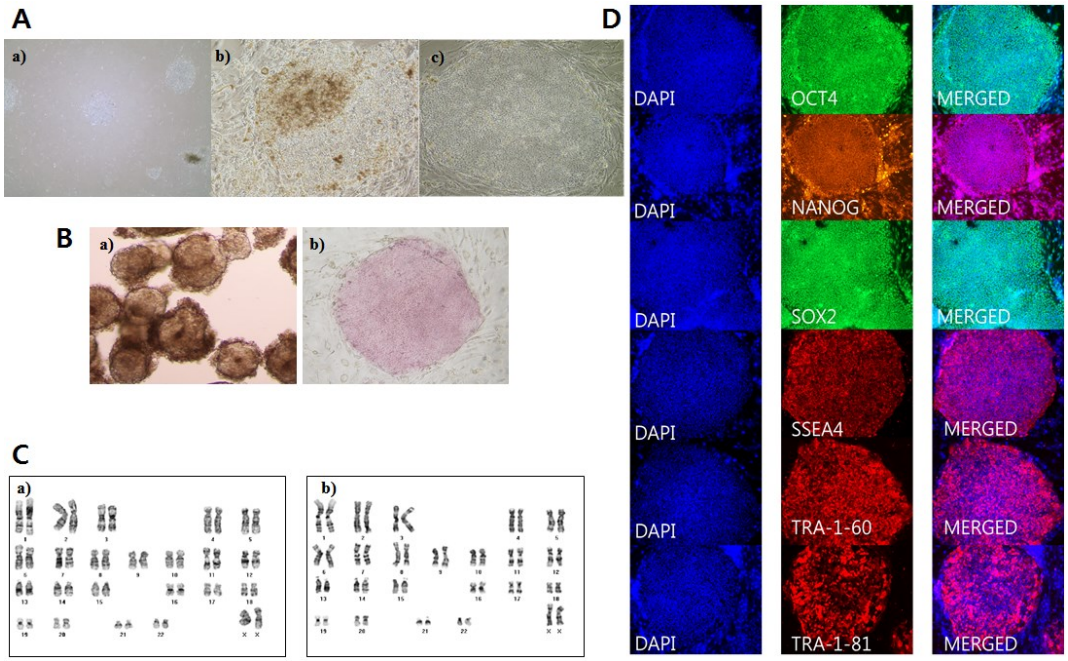

Figure 1. Characterization of hGF-derived iPSc. (A) Morphology of gingival fibroblast-iPScs (a) Human gingival fibroblast 2 days after Sendai virus transduction (b) ES cell-like colonies after 7 days post transduction (c) more prominent ES cell-like colonies after 14 days post transduction. (B) (a) Embryonic body formation (b) ES cell-like colonies stained with alkaline phosphatase. (C) Karyotyping of human gingival fibroblast-iPScs (a) karyotyping for gingival fibroblast (b) chromosomal analysis revealed a normal karyotype for human gingival fibroblast-iPScs. (D) Expression of human embryonic stem (ES) cell-associated proteins by gingival fibroblast-iPScs; OCT4, NANOG, SOX2, SSEA4, TRA-1-60, TRA-1-81 expression were shown. 4-6-Diamidino-2-[henylindole (DAPI) was used as blue nuclear staining control

To examine the pluripotency of hGF-iPSc, we performed *in vitro* differentiation analysis followed by EB formation. 14 days post EB culture, expression of lineage-specific markers a-fetoprotein, brachyury and b-tubulin for endoderm, mesoderm and ectoderm, respectively were analyzed by immunocytochemistry. (Fig2A) Also, increased lineage-specific gene expression was identified through the quantitative real-time PCR gene expression results. (Fig2B)

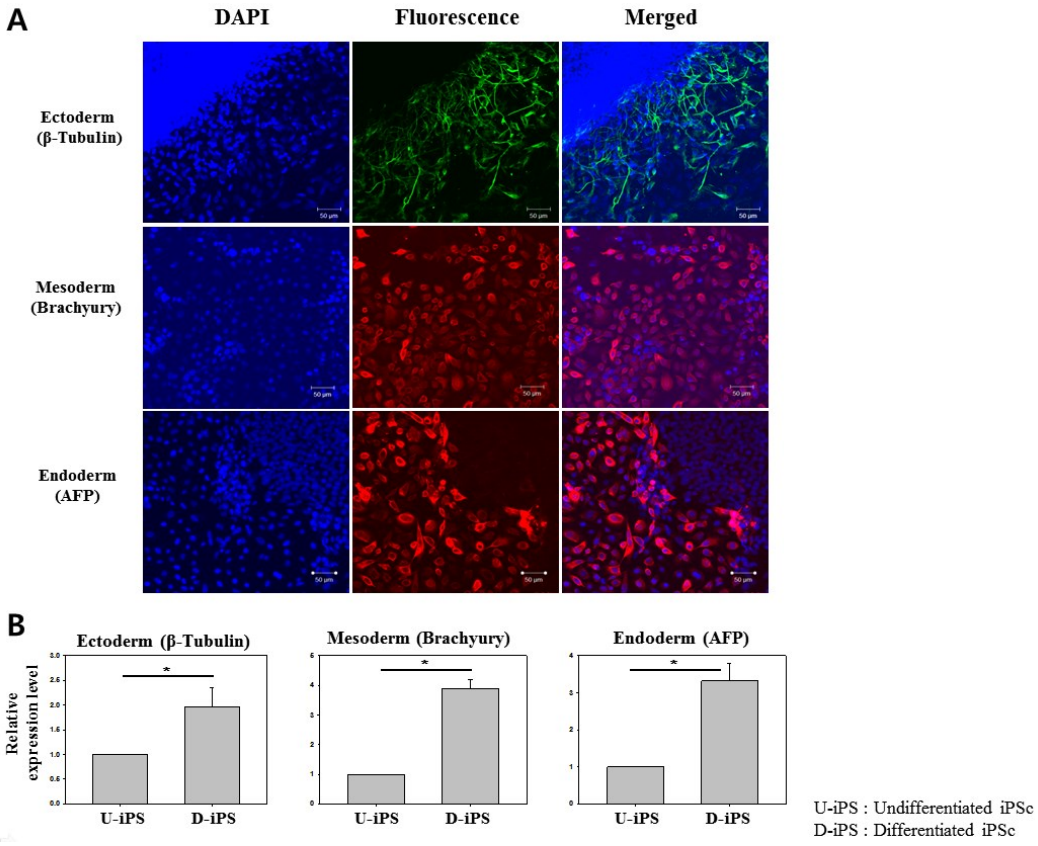

Figure 2. In vitro 3-germ layer differentiation of hGF-iPSc. (A) Expression of lineage-specific markers a-fetroprotein, brachyury and b-tubulinIII for endoderm, mesoderm and ectoderm, respectively by immunocytochemistry (14 days post EB culture), (B) lineage-specific gene expression obtained from qRT-PCR results.

***in vitro* differentiation of iPSc derived from dental stem cell**

For detection of calcium deposition, Von Kossa staining revealed osteogenic activity with mineralized nodule formation in hGF-iPSc and this was re-confirmed by the strong alizarin Red S staining and gene expression. (Fig3A) (Fig3B) RT-PCR gene expression revealed that pluripotent marker, OCT4 decreased in osteogenic differentiated iPSc whereas osteogenic marker, RUNX2 conversely increased in osteogenic differentiated iPSc. (Fig3B)

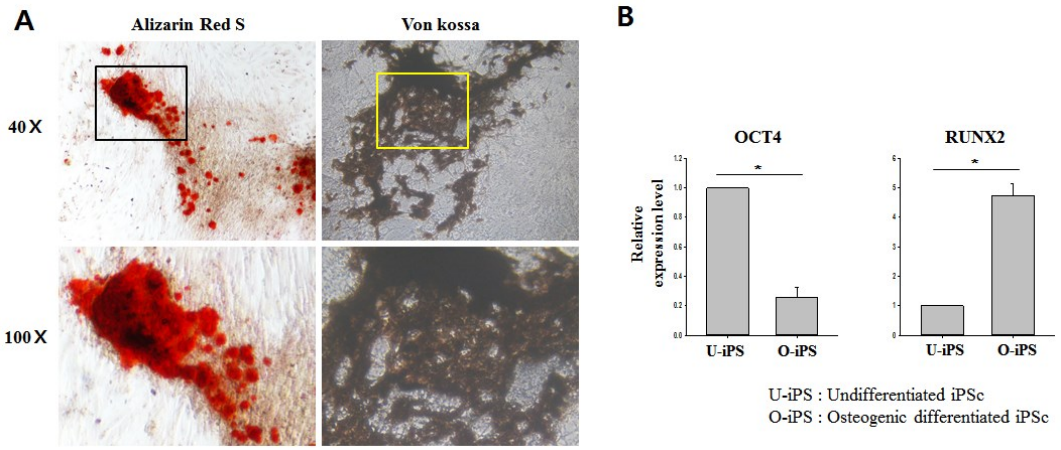

Figure 3. Osteogenic differentiation of hGF-iPSc. (A) Alizarin Red S Staining (40 , 100) and Von kossa staining, (B) OCT4 and RUNX2 gene expression level of UiPS and O-iPS.

Alizarin Red quantification of osteogenic differentiation

To confirm the differentiation capacity of hGF-iPSc on titanium disc, osteogenic differentiation was induced. Mid- to long-term culture (14 to 28 days) of hGF-iPSc under the osteogenic media demonstrated significantly increased capacity to form Alizarin Red-positive compacted nodules with high levels of calcium deposition on both cell culture plate and titanium disc compared to undifferentiated hGF-iPSc. (Fig4A) In particular, osteogenic induced hGF-iPSc on SLA-treated titanium disc displayed the greatest level of calcium deposition measured at 14 days post treatment. However, measurement recorded at 28 days post-treatment showed no significant difference, showing the similar level of calcium deposition regardless the type of culture surface. (Fig4B)

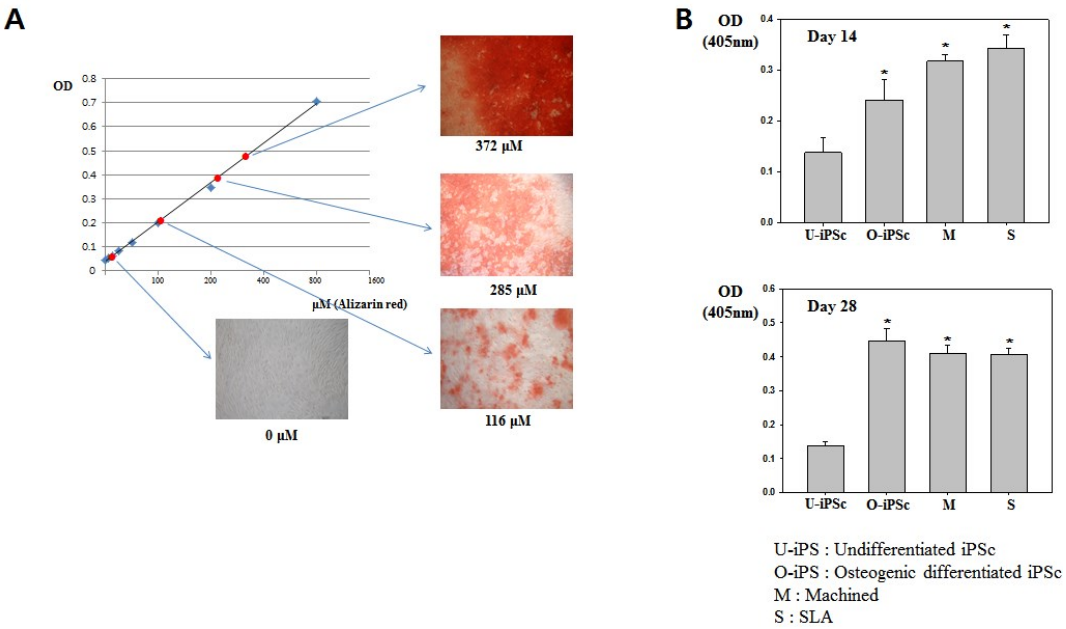

Figure 4. Alizarin Red quantification of osteogenic differentiation. (A) Alizarin Red S standard curve. (B) Quantitative results of the Alizarin Red staining measured at day 14 and day 28

SEM analysis

The surface of machined and SLA titanium disc clearly showed the difference in cell morphology and surface characteristics. The untreated machined surface titanium disc showed a relatively flat topography while SLA titanium disc showed relatively rougher surface with shallow pits. hGF-iPSc on both surfaces adhered well from Day 1 and significant 'filopodia cell attachment' of hGF-iPSc was found on SLA-treated surface up until 7 days after seeding, spreading in different layers over the whole rough surface. There was no significant difference in cell number between two groups although reduced cell numbers were observed after Day 14 in both groups. The crystalline structure on machined surface appeared on 14 days after seeding and became even more significant on Day 28, indicating the differentiation into osteoblast-like cells. In contrast, no crystalline structures were identified on SLA-treated surface. (Fig5)

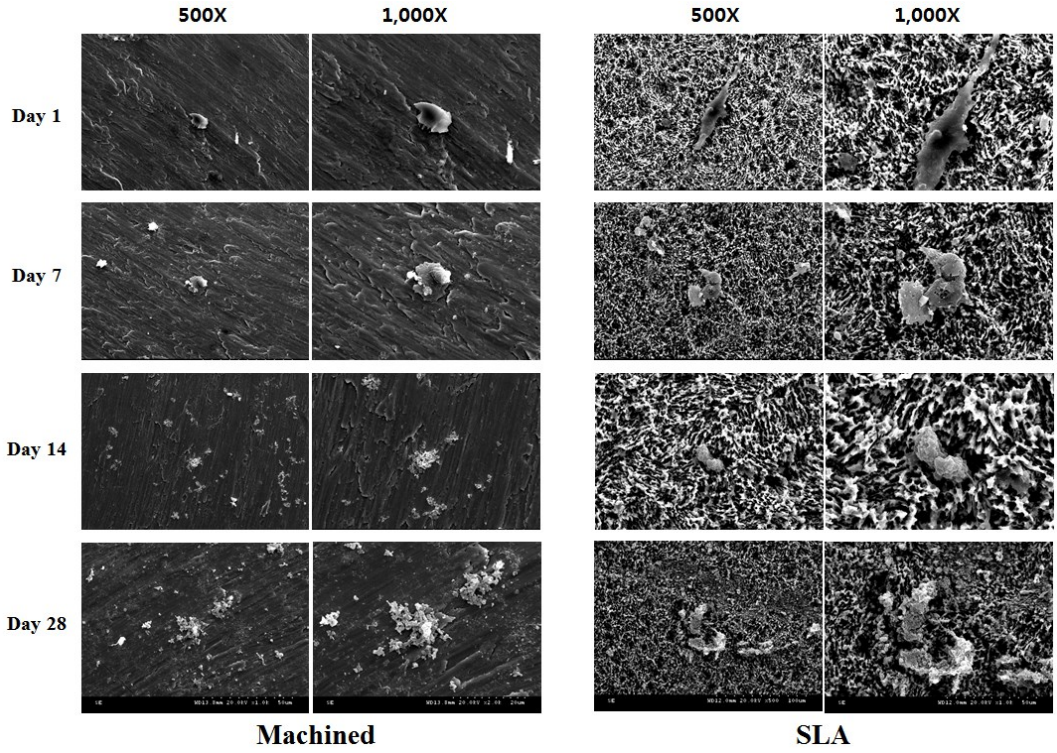

Figure 5. SEM images of hGF-iPSc cultured with osteogenic media on Machined- and SLA-treated titanium surfaces at 1,7,14 and 28 days after initial culturing.

Expression of osteogenic genes of iPSc (flow cytometry analysis and RT-PCR)

The results from flow cytometry analysis revealed that osteogenic marker, Osteocalcin, was significantly increased in osteogenic differentiated hGF-iPSc, hGF-iPSc cultured on machined disc and SLA-treated disc compared to that of undifferentiated hGF-iPSc, confirming successful osteogenic differentiation of hGF-iPSc on both cell culture plate and titanium disc. (Fig6A)

The expression of osteogenic genes including COL1, RUNX2, IBSP and BGP of hGF-iPSc cultured on differently surface-treated titanium disc were evaluated by qRT-PCR analysis on specimens collected after 14 days and 28 days of initial cell culture. Expression levels were evaluated versus a control consisting of hGF-iPSc cultured on conventional cell plate as well as hGF-iPSc cultured without osteogenic induction medium. It was clearly noticed that hGF-iPSc cultured on surface- treated titanium disc, measured at both 14 and 28 days post cell culturing, demonstrated the greater bone-related gene expression than hGF-iPSc cultured on conventional cell plate. However, when comparing gene expression between SLA-treated titanium disc and machined titanium disc, SLA-treated titanium disc showed statistically significantly increased gene expression.(COL1, RUNX2). Although statistically not significant, IBSP and BGP expression of hGF-iPSc culture on SLA-treated titanium disc also found to be greater than machined titanium disc. In addition, it was also identified COL1 and RUNX2 expression, measured at 14 days of initial cell culture, and was rather decreased on machined titanium disc compared to hGF-iPSc cultured on conventional cell plate. (Fig6B)

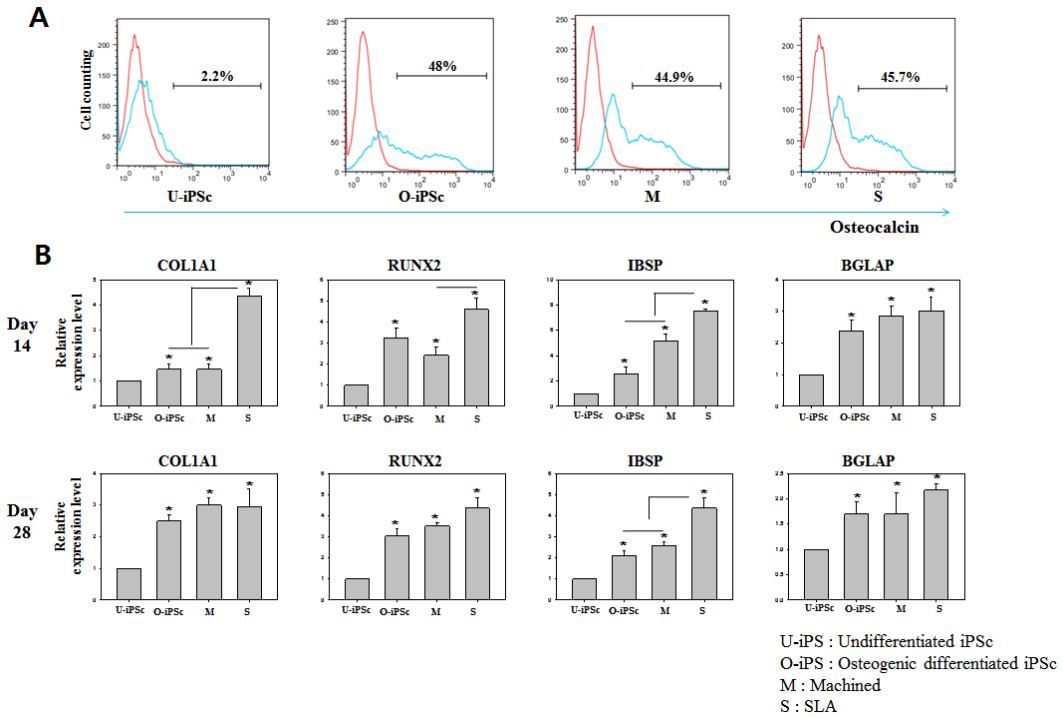

Figure 6. Molecular quantification of osteogenic differentiation. (A) Flow cytometric analysis (Osteocalcin marker expression) (B) RT-PCR results (Day 14 and Day 21) of U-iPSc (Control), iPSc-derived osteoblast (O-iPSc), iPSc cultured on SLA surface (S) and iPSc cultured on machined surface (M)

Ⅳ. DISCUSSION

The ability to control the fate of stem cell is of major relevance in regenerative dentistry as well as tissue engineering, providing more rational approach for the design of next-generation implants. In particular, osteogenic response from these stem cells is favorably desired, stimulating rapid new bone formation and enhanced osseointegration, which will, in turn, lead to increase early stage stability of the implant, reducing in healing times after implantation. It is now well accepted that implant surface topographies ranging from nano- to micros scale have a significant impact on cellular attachment, proliferation and even differentiation and consequently, there has been several studies investigating the effect of surface topography on the fate of different stem cells including MSCs which has been used as a gold standard for regenerative medicine.(21, 22) However, very few studies reported bone regeneration by osteogenic response from iPSc derived from dental stem cells although iPSc showed a greater possibility of being utilized in many aspects over MSCs as aforementioned. Therefore, in this study, we aim to evaluate investigate the behavior of iPSc derived from dental stem cells in terms of initial adhesion, differentiation potential using differently surface-treated titanium disc.

In this study, we demonstrated the generation of iPSc lines from hGF using the Yamanaka cocktails as previously reported.(23) The established hGF-iPSc share the similar characteristics with the ES cells as shown in the results of the current study; a strong AP activity, the same pluripotent stem cell markers (OCT4, NANOG, SOX2,

SSEA4, TRA-1-60, TRA-1-80) detected, possession of pluripotency to differentiate into three germ layers (endoderm, mesoderm and ectoderm), and normal karyotyping. We also observed strong osteogenic activity of hGF-iPSc observed by Alizarin red S and Von Kossa staining. Although, Yan et al. reported that hGF other than other dental stem cell lines were poor cell sources to reprogram into iPSc, judging from the results of the current study, we have confirmed that hGF could be efficient cell sources for the generation of iPSc, thereby suggesting that hGFs are good alternative sources for iPSc banking in replacement of bone marrow stem cell due to easy accessibility during simple, routine dental treatment. Also, while many other multiple adult stem cell lines taken far away from dental origin only shows limited potential, iPSc was reported to contain an epigenetic memory of their tissue of origin, contributing to a greater differentiation potential into desired cell lineage.(24) Therefore, it can be suggested that our studies using iPSc derived from dental stem cells represent the significant advancement in utilizing patient-specific tissue regenerative treatment for implant or implant-related disease. Nevertheless, due to the use of viruses during the cell reprogramming process, safer application of iPSc to clinic has been very limited. Therefore, the importance of further study investigating long-term behavior of iPSc for clinical application cannot be more emphasized.

In this study, we also aimed to evaluate the behavior of iPSc derived from dental stem cells depending on different surface characteristics. Based on the previous studies indicating there is a strong correlation between early cell response to surfaces and cell's behavior, behavior of hGF-iPSc in terms of initial adhesion, differentiation potential

were investigated. The results from SEM analysis revealed that the surface of machined and SLA titanium disc clearly showed the difference in cell morphology and surface characteristics. Although hGF-iPSc cultured on both surfaces seemed to be adhered well from Day 1, philophodia cell attachment of hGF-iPSc was found on SLA-treated surface up until 7 days after seeding, adhering more tightly over the entire rough surface. While the presence of influences of the surface topography to bone response at the cellular level is considered controversial, it is generally accepted that the rougher implant surface, the more active cellular response in terms of adhesion and differentiation into osteoblast.(25, 26) Inzunza et al. (27) reported that early osteoblast adhesive response was accelerated on the rougher nano-porous coated structure, promoting osteogenic differentiation of mesenchymal stem cell with spontaneous mineral nodule formation. It was also reported that embryonic stem (ES) cell also showed increased osteogenic differentiation and increased expression of collagen type I, RUNX2 and osteocalcin when cultured on rougher nano-surface modified scaffold.(28) Therefore, it may be anticipated that iPSc, which shares the similar characteristic with ES cell represent similar cellular response to the certain surface morphology and this was confirmed by the quantitative RT-PCR results of the current study. The quantitative RT-PCR results clearly revealed that COL1 and RUNX2, indicative of early osteogenic markers, were significantly increased with hGF-iPSc culture on the SLA-treated titanium disc compared to machined titanium disc.($p<0.05$) Also, the level of IBSP and BGP were greater in iPSc cultured on the SLA-treated titanium disc although significance between two groups was not found ($p>0.05$). These results were in accordance with previous study, investigating the effect of surface

type on osteogenic differentiation potential of human MSCs. (29) Although cell lines investigated were different, multiple osteogenic makers including Alkaline phosphatase(ALP), and Osteocalcin(OC), Osteoprotegerin(OPG) and Transforming growth factor beta 1(TGF-b1) were significantly increased with MSCs cultured on the SLA-treated surface.(29-31) Therefore, we can assume that this result is particularly meaningful, since our results displayed promising results with iPSc by replicating the results from MSCs, showing the potential use of hGF-iPSc in the field of cell-based bone tissue engineering. As MSCs have been regarded as a key cell type required for osseointegration and bone healing [6][7], the results of this study clearly demonstrated that even iPSc which can circumvent the disadvantage MSC can also be utilized as standard treatment modality for possible reduction in healing times after dental implantation. Indeed, further study investigating the anti-inflammatory effect of differentiated iPSc in order to improve the potential use of iPSc in clinic and comparing the level of osseointegration with MSCs *in vivo* to confirm the iPSc as a new treatment modality for implant-related disease may be required.

Ⅴ. CONCLUSION

Within the limitation of the study, our study clearly represents that behavior of iPSc derived from dental origin can be directed by implant topographic change, indicating potential use of iPSc derived from dental origin as patient-specific tissue regenerative treatment modality for dental implant or implant-related disease.

Chapter 2

In vivo study for clinical application of dental stem cell therapy incorporated with dental implant

ABSTRACT

In vivo study for clinical application of dental stem cell therapy incorporated with dental implant

Purpose The aim of this study is to investigate the behavior of dental derived human mesenchymal stem cells (d-hMSCs) in response to differently surface-treated implant and to evaluate the effect of d-hMSCs on local osteogenesis around an implant *in vivo*.

Methods d-hMSCs derived from alveolar bone was established and cultured on machined- and Sandblasted and acid etched (SLA)-treated titanium disc with and without osteogenic induction medium. Their morphological and the level of osteogenic potential were assessed by scanning electron microscopy (SEM) and real time polymerase chain reaction (RT-PCR). 5 x 10^6 of d-hMSCs was mixed with 1ml of Metrigel and 20μl of gel-cell mixture were dispensed into the defect followed by the placement of customized mini implants (machined-, SLA-treated implants) in New Zealand White rabbits. Following healing period of 2 weeks and 12 weeks, the obtained samples in each group were analyzed radiographically, histomorphometrically and immunohistochemically.

Results Quantitative change in osteogenic differentiation of d-hMSCs was identified according to the type of surface treatment. Radiographic analysis revealed that increase in new bone formation was statistically significant in d-hMSCs group. Histomorphometric analysis was in accordance with radiographic analysis, showing the

significantly increased new bone formation in d-hMSCs group regardless of time of sacrifice. Human nuclei A was identified near the area where d-hMSCs were implanted but the level of expression was found to be decreased as time passed.

Conclusion Within the limitation of the present study, in this animal model, the transplantation of d-hMSCs enhanced the new bone formation around an implant and the survival and function of the stem cell was experimentally proved up to 12 weeks post sacrifice.

Keyword : *dental derived human mesenchymal stem cells, titanium disc, rough surface, osteogenesis, animal study*

Ⅰ. INTRODUCTION

The establishment of osseointegration is one of the key factors for the long-term success of oral implant and many previous studies reported that osseointegration can be manipulated and improved by changing implant surface properties. (25) It is generally accepted that rough surface promotes osseointegration more effectively than machined surface by providing an increased surface area for cell attachment, resulting from an increase in the production of Prostaglandin E2 and TGF-b1, where are known to promote osteoblast differentiation, leading to enhanced subsequent bone formation. (32, 33) Consequently, mechanical and chemical surface treatments including sand blasting and acid (SLA) (34), anodization, (34) hydroxyapatite coating, (35) plasma treatment, (36) UV photofunctionization (37, 38) have been used successfully used to modify the titanium implant surface.

Recently, with the advancement of tissue engineering technique, many researchers have attempted to better understand the biological reaction underlying cell to implant surface. Since human mesenchymal stem cells (hMSCs) have shown potential in the treatment of many disease including inflammatory disease (39), diabetes (40), myocardial infarction (41) and liver cirrhosis (42), hMSCs have also been identified as a key cell type required for osseointegration and bone remodeling. (43, 44) Although several investigators have evaluated the effect of implant surface treatment on osteogenic differentiation of hMSCs in vitro, (45-48) there have been less extensive in vivo literature on the fate of hMSCs on

differently surface treated implant for clinical application. Moreover, although it has been widely recognized that hMSC obtained from dental origin has higher proliferation and osteogenic differentiation capacity compared with those in hMSCs obtained from iliac crest, functional differences depending on origin of the cell source have been overlooked in many previous studies. Indeed, it can be anticipated that greater knowledge regarding the fate of hMSC, especially hMSCs obtained from dental origin, on implant surface could lead to greater clinical implant success and further understanding of the underlying mechanisms governing the fate of d-hMSCs.

Therefore, the aim of this study is to investigate the behavior of d-hMSCs in response to differently surface-treated implant and to evaluate the effect of d-hMSCs on local osteogenesis around an implant *in vivo.*

Ⅱ. MATERIALS AND METHOD

In vitro analysis

Titanium surface preparation

In brief, titanium discs (Dentium Co., Ltd, Seoul, Korea) with dimension of 10mm diameter and 2mm thickness were fabricated using commercially pure titanium alloy and either machined or sandblasted with large grits and acid etched (SLA)-treated, ready to be used for the cell. Prior to usage, all discs were thoroughly washed with distilled water, dried and sterilized with Ethylene Oxide (EO) gas.

Cell preparation

The experiment was approved by the Institutional Research Ethic Committee of the Yonsei University College of Dentistry. (IRB NO.14-0097) human alveolar bone marrow from mandible were obtained from healthy subjects (aged: 19-40 years old) who visited the Yonsei University Dental Hospital. To obtain d-MSCs, alveolar bone marrow aspirates (0.5–1.0 mL) were collected from osteotomy sites during implant surgery using an 18-gauge needle syringe without contamination of periodontal tissues. Stromal cells including erythrocytes were seeded at a 100-mm tissue culture dish (BD, Pharmingen, CA, USA) and maintained in 15 ml of DMEM supplemented with 10% FBS (Gibco, Invitrogen Corporation, Grand Island, NY, USA) and antibiotics (100 units/ml penicillin

G and 100 μg/ml streptomycin). Three days after seeding, floating cells were removed, and the medium was replaced by fresh medium. Attached cells were fed with fresh medium, which was added every other day. Subsequent passages were performed when cells were approaching confluence. Each cell at passages P3-P4 was used for the characterization and further evaluation. Characterization process involved immunocytochemical analysis, cell-surface-marker characterization, and induction of osteogenic differentiation to test if d-hMSCs possess the basic characteristics of mesenchymal stem cells. (Data not shown)

Surface analysis by SEM

The samples were examined using a scanning electron microscope (SEM, Hitachi, S-800, Japan) at 15Kv accelerating voltage. The samples were initially fixed in 2% paraformaldehyde buffer, rinsed, dehydrated in graded alcohol and dried. The samples were then photographed at 1, 5, 7 days after initial culturing for 2 days followed by culturing in osteogenic-conditioned media containing β-GP, dexamethasone, ascorbic acid and their time-dependent and surface-dependent morphological changes were analyzed with a fully computerized high-resolution SEM at three different magnification levels (1:12, 1:1000 and 1:3000).

Flow cytometer analysis

d-hMSCs were detached from the culture dish using Triple express solution (Invitrogen, Waltham, MA, USA), centrifuged, rinsed and re-suspended in PBS at a concentration of 1 x 10^5 cells/mL. Re-suspended cells were incubated with 5 μL of fluorescein isothiocyanate-labled anti-rat human osteocalcin (BD), in the dark at 4 C for 30 min. After being washed twice with PBS, cytometric analysis was performed using a flow cytometer (BD FACS Verse)

Quantitative RT-PCR

Total RNA was isolated using RNA RNeasy kit (Qiagen, Valencia, CA, USA).The quality of the RNA was evaluated using spectrophotometry and denaturing agarose gel electrophoresis. cDNA was synthesized from 1 μg of purified total RNA using a PrimeScript RT reagent kit (Invitrogen), according to the manufacturer's instructions. The used primer sequences were described in Table 1. Quantitative RT-PCR analysis was performed with SYBR green real-time PCR master mix (Thermo Fisher scientific, Waltham, MA, USA) in a 7500 Real-Time PCR System (Thermo Fisher scientific). The PCR conditions were 95°C for 30 s, 40 cycles of denaturation at 95°C for 5 s and annealing and extension at 60°C for 15 s, followed by dissociation and a standard denature action curve.

Gene name	Gene ID	sequences	Amplicon length(bp)
Human GAPDH F	M33197.1	cgaccactttgtcaagctca	203
Human GAPDH R		aggggagattcagtgtggtg	
Human IBSP F	NM_004967.3	cgccaatgaatacgacaatg	196
Human IBSP R		gatgcaaagccagaatggat	
Human COL1A1 F	NM_000088.3	ggcccagaagaactggtaca	200
Human COL1A1 R		cgctgttcttgcagtggtag	
Human BGLAP F	NM_199173.4	ggcagcgaggtagtgaagag	194
Human BGLAP R		agcagagcgacaccctagac	
Human RUNX2 F	NM_001015051.3	agtgccagctgcatcctatt	201
Human RUNX2 R		tgcttgaatttttcccaagg	

Table 1. RT-PCR primer information

In vivo analysis

Preparation of customized implant

Non-threaded type Customized implant (Dentium Co., Ltd, Seoul, Korea) with a diameter of 1.5mm and height of 3.7mm are designed and surfaced treated. (machined- or SLA treated-)

Animal preparation and in vivo d-hMSC transplant

Twenty New Zealand white rabbits, 6 weeks old weighting 4.0kg each, were used in this study. Animal selection, management, surgical protocol, and procedures for this study were reviewed and approved by the Institutional Animal Care and Use Committee, Yonsei Medical Center, Seoul, Korea. (Approval no. 2013-0347-2) All surgical procedures were performed under general anesthesia. The animals were anesthetized with intravenously administered mixture of 30 mg/kg of Zolazepam (Zoletil Virback

Korea Co., Seoul, Korea) and 10 mg/kg of Xylazine HCI (Rumpun, Bayer Korea, Seoul, Korea). After ten minutes, the site of surgery was shaved and sterilized with povidone-iodine and then further anesthetized with 2% lidocaine HCl with epinephrine 1 : 80000 by infiltration. The defect size with 1.0mm in diameter and 4mm in height were made using dental diamond bur and customized implants were placed in the right and left tibia of rabbit. According to the study design, 5 x 10^6 d-hMSCs were mixed with 1ml of Metrigel^{TM} (BD) and 20μl of gel-cell mixture were dispensed into the defect prior to implant placement. 2, 12 weeks post implantation animals were sacrificed by 2% paraformaldehyde injection to heart under a general anesthetic. (Fig1) Then, the block sections including implants were preserved and fixed in 10% neutral buffered formalin for 2 weeks. The obtained samples in each group were analyzed radiographically, histomorphometrically and immunohistochemically.

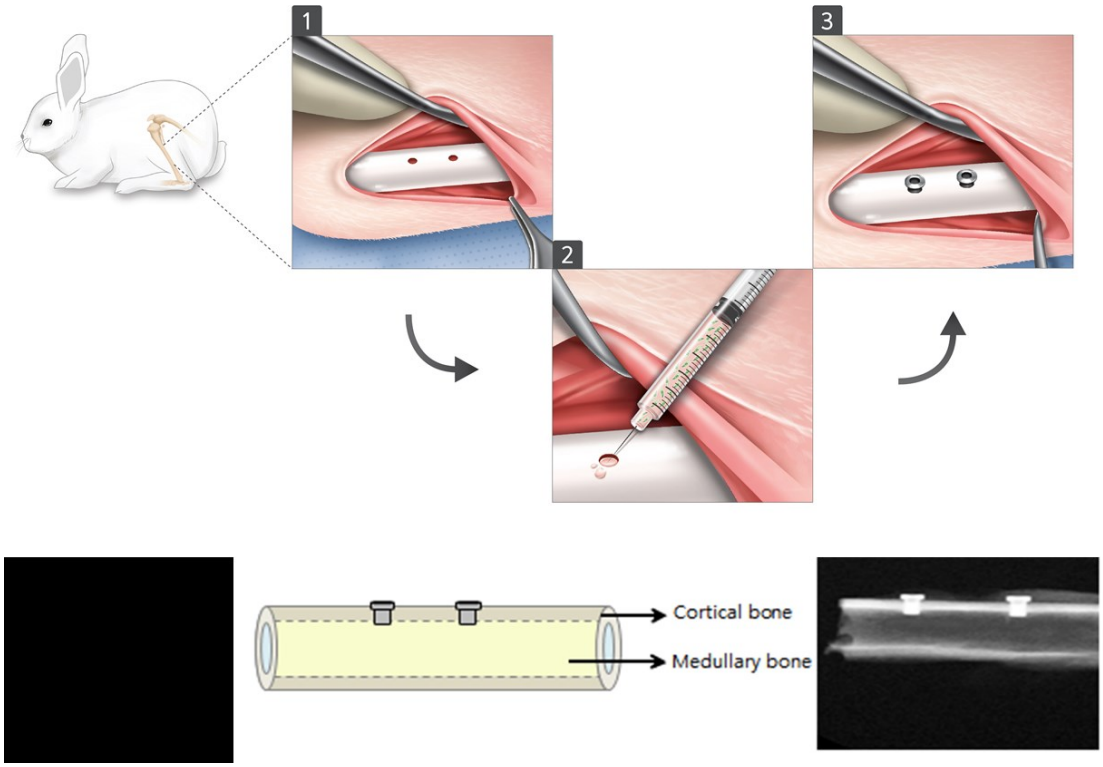

Fig1. Surgical procedure used in this study

Radiological analysis

New bone volume was determined at two points from plain x-ray images: (a) new bone volume (μm x μm) formed from the implant head; upper (b) new bone volume (μm x μm) formed from the apical portion of the implant; lower. (Fig2) Each measurement was performed by one experienced examiner using specific image software (Image-Pro Plus, Media cybernetics, Silver Spring, Maryland, USA). 3D images of the samples were reconstructed and the amount of new bone formation around implants were measured within Region of interest (ROI) box using micro-computed tomography scanner(SkyScan 1076, Skyscan, Aartselarr, Belgium) at a resolution of 35um(achieved using 100kV and 100uA).). ROI box was set with dimension of 1.30mm (x axis) x1.30mm (y axis) x 0.45mm (z axis). (Fig3)

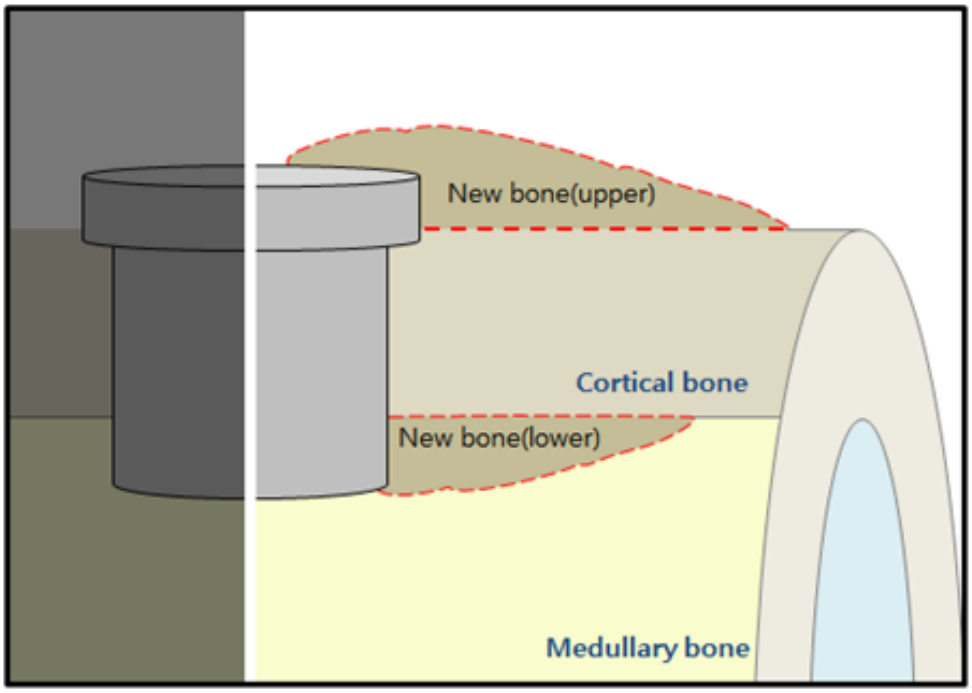

Fig2. Schematic diagram depicting the measuring parameters (newly formed bone: upper and lower)

Histological & histomorphometric analysis (H&E, Russell-Movat pentachrome: bone volume, bone-implant contact)

The specimens were dehydrated through graded alcohols of 70%, 80%, 95%, and 100% at 2 h intervals for 1 week. The specimens were then embedded in Technovit 7200 (Heraeus Kulzer, Dormagen, Germany) and alcohols (1 : 3, 1 : 1, and 3 : 1 ratio) and sectioned in the buccolingual plane using a diamond saw (Exakt 300, Kulzer, Norderstedt, Germany). From each implant site, the central section was reduced to a final thickness of about 15 μm by micro grinding and polished with a cutting-grinding device (Exakt 400CS, Exakt Apparatebau, Norderstedt, Germany) and finally stained with hematoxylin and eosin (H&E) and Russell-Movat pentachrome stain. (American Master Tech, Lodi, CA, USA) The stained specimens were captured using light microscope (Leica DM 2500, Leica Microsystems, Wetzlar, Germany) at x12.5, x50 and x100 magnification. The new bone volume (BV) and new bone-implant contact (BIC) within ROI box around the implants were measured using imaging analyses system (Image-Pro Plus 4.5 Media Cybernetics Inc., Silver Springs, MD, USA). ROI box was set with dimension of 1.30mm (x axis) x1.30mm (y axis). (Fig3)

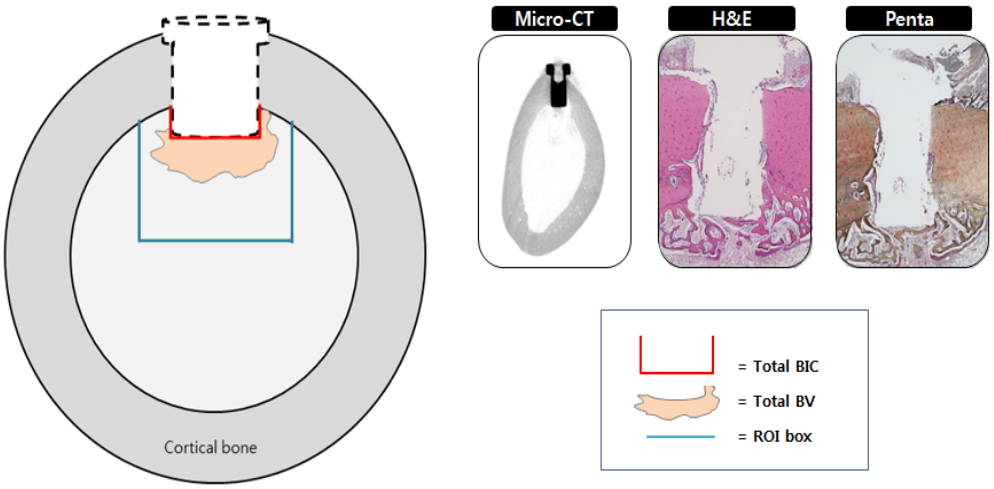

Fig3. Method of measuring the bone-implant contact (BIC) value and newly formed bone area within Region of interest (ROI)

Immunohistochemistry (Human nuclei A, BrdU)

Immunohistochemistry analysis was conducted according to previously reported study. (49) Briefly, paraffin samples were de-paraffinized and hydrated. Then, antigen retrieval was carried out with Sodium citrate buffer (10 mM Sodium citrate, 0.05% Tween 20, pH 6.0). The endogenous hyperoxidase was blocked with0.3% H_2O_2 in PBS. After incubation of the sections in blocking buffer, all the bound antibodies were detected using biotinylated anti-mouse or anti-rabbit secondary antibodies, followed by the addition of complex avidin-peroxidase. Counterstaining was performed with haematoxylin. Antibody dilutions used in this study are as follows: Human nuclear A antigen 1:25 (ab191181, Abcam, Cambridge, MA, USA).

Statistical analysis

The results from the radiological, histomorphometrical, immunohistochemical analysis were expressed as the means+SDs and difference between groups were analyzed using SPSS (version23.0, IBM Corporation, Armonk, NY, USA). Statistical significance was analyzed by one-was ANOVA. Post-hoc Duncan's multiple-range test was used to identify statistically significant difference, with a significance level of 5%.

Ⅲ. Results

In vitro analysis

Surface analysis by SEM

The surface of machined- and SLA- titanium disc clearly showed the difference in cell morphology and surface characteristics. SEM analysis showed that d-hMSCs seemed to be adhered well across the whole surface from Day 1 regardless of the surface type and use of osteogenic induction media (Fig4). From day 5 of culture, individual d-hMSCs under osteogenic condition and d-hMSCs cultured on SLA surface cannot be discerned as SEM images revealed the progressive deposition of the matrix, characterized by the appearance of circular nodule formation and decrease in cell number. By day 7 of cell culture, the basal surface of the titanium disc was covered by the cell population and evidence of mineralized crystalline-like structure became more evident. This appearance was clearly distinguishable from that of the cells cultured on machined surface without osteogenic induction media.

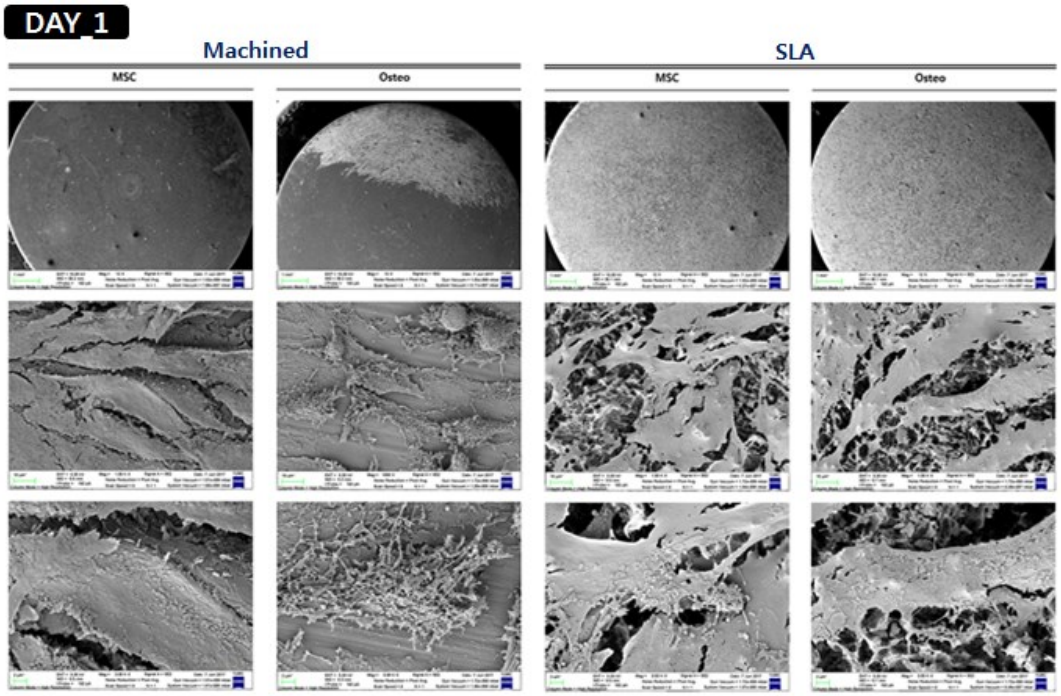

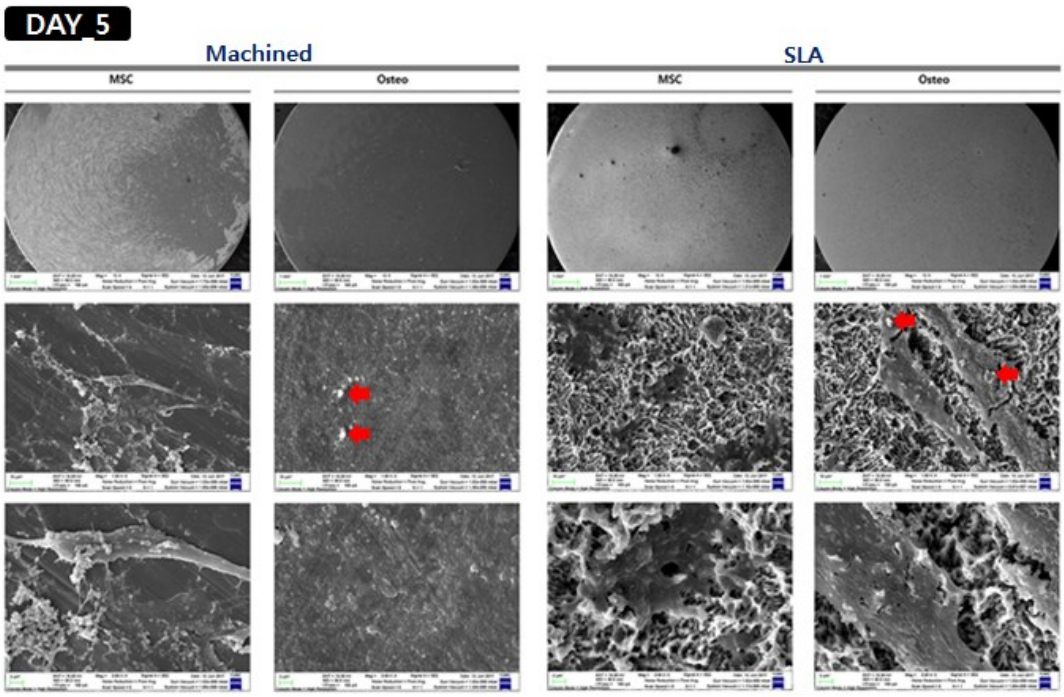

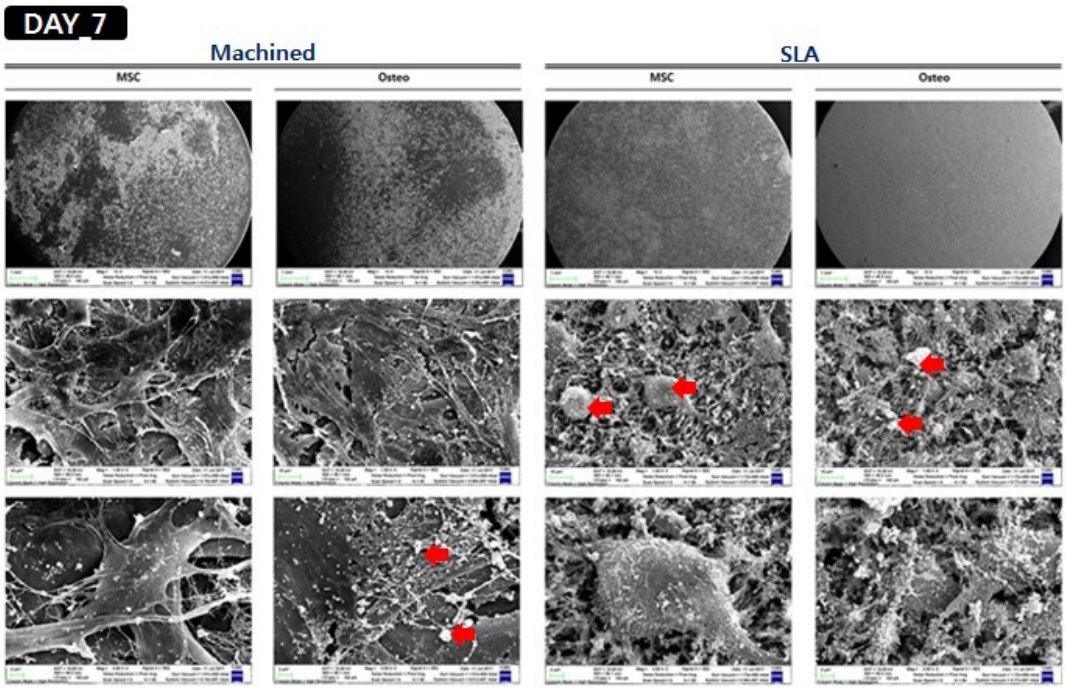

Fig4. SEM images of dental derived hMSCs cultured with osteogenic media on Machined- and SLA-treated titanium surfaces at 1,5,7 days after initial culturing. (Red arrows indicates mineralized crystalline-like structure)

Expression of osteogenic genes of d--hMSCs (RT-PCR)

The expression of osteogenic genes including COL1, RUNX2, IBSP and BGP of d-hMSCs cultured on differently surface-treated titanium disc were evaluated by RT-PCR analysis on after 7 days and 28 days of initial cell culture. d-hMSCs cultured on conventional cell plate were used as a control to normalize the results obtained in the RT-PCR analysis. From the results of Day 7, it was clearly noted that d-hMSCs cultured on SLA titanium disc demonstrated the greater bone-related gene expression than d-hMSCs cultured on conventional cell plate and machined titanium disc although there was no statistically significant difference among the groups. ($p>0.05$) On the other hand, COL1, representative early osteogenic marker, was rather lesser in SLA surface than machined surface, suggesting progression of osteogenic differentiation. Although statistically not significant, IBSP and BGP expression of d-hMSCs culture on SLA-treated titanium disc was also found to be greater than machined titanium disc 28 days after initial cell culture. ($p>0.05$) (Fig5)

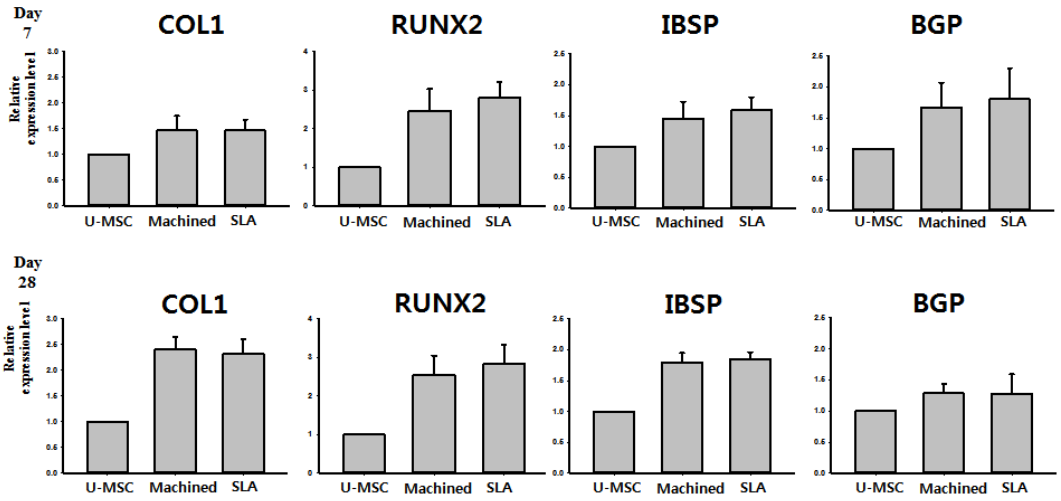

Fig5. Molecular quantification of osteogenic differentiation of d-hMSCs on either cell plate (undifferentiated MSC, U-MSC), machined-(Machined) or SLA-surface (SLA) titanium disc.

In vivo analysis

Radiological analysis

As aforementioned, new bone volume (μm^2) was determined at two points from plain X-ray images; (a) upper (b) lower. At 2 weeks, the new bone volume (upper) measured in control group of SLA surface was rather greater than that of d-hMSCs group, showing the negative effect of d-hMSCs on new bone formation. However, in 12 week group, such negative effect had been compensated, showing that d-hMSCs group demonstrated greater new bone volume than control group regardless of the surface type. ($p>0.05$)

On the other hand, the new bone volume measured in lower part of implant (lower), the area in which the cells are most prone to be active due to the orientation of injection, displayed greater new bone formation in d-hMSCs group at both 2 week and 12 week. In particular, when comparing new bone volume (lower) measured from SLA surface of control group and d-hMSCs group, d-hMSC group showed statistically significantly greater new bone volume than control group. ($p<0.05$)

Micro CT results which measured new bone volume within ROI region are in accordance with the results of the measurement from plain x-ray images. Although statistically not significant, d-hMSCs group at 12 weeks demonstrated a greater new bone volume than control group regardless of the surface type. (Fig6)

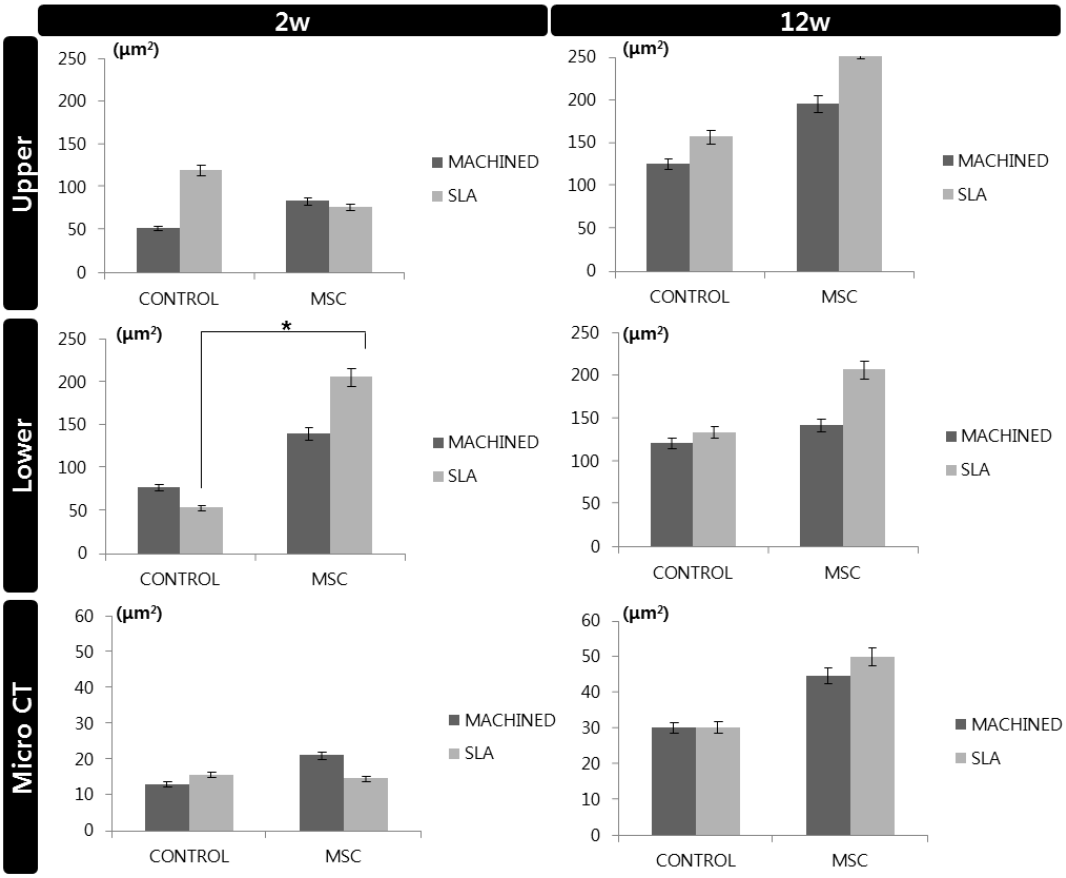

Fig6. Newly formed bone (upper and lower) measured from x-ray images and within ROI from micro CT images.

Histological & histomorphometric analysis (H&E, Russell-Movat pentachrome: BIC, BV)

None of the animals used in this study exhibited excessive inflammation, maintaining a healthy condition. Therefore, all samples were included for micro CT, histologic and histomorphometric analysis.

At 2 weeks, regardless of the surface type of implant, a new bone interface connecting the surgically created defect was observed in d-hMSCs group as a form of elongated bone cluster mixed with fibrocartilaginous callus-like tissue whereas the clear defect margin was maintained in control group, showing no sign of new bone formation along the defect margin. In control group, large amount of bubble-shaped adipose tissue consisting of many small droplets were identified below the defect margin and within the bone marrow. However, in d-hMSCs group, this area filled seemed to be replaced by extensive woven bone network, bridging from one side to the other side. There was no sign of immune response which may have resulted from heterogeneous human cell injection. (Fig7)

At 12 weeks, more prominent continuous new bone formation was observed in the d-hMSCs group, showing complete ‘bridging’ of the defect. The bony bridge consists of lamellar bone, characterized by consistence alignment of osteocyte. However, the thickness and quality of new bone did not seem to be different according to surface type. Conversely, the defect margin without d-hMSCs engrafting still showed opening of the

defect, although very small amount of new bone formation was observed near the defect margin. Also, amount of adipose tissue which was abundantly found in 2-week group, has dramatically reduced in all groups and dense connective tissue was no longer identified. (Fig7)

The results of the histomorphometric analysis are summarized in Figure 8. The average BIC values measured within ROI for control group (machined, SLA) were 375.25 (μm^2) and 343.57(μm^2) at 2 weeks, and 402.78 (μm^2) and 486.34 (μm^2) at 12 weeks, respectively. The average BIC values measured within ROI for d-hMSCs group (machined, SLA) were 613.03 (μm^2) and 597.03 (μm^2) at 2 weeks, and 655.67 (μm^2) and 855.69 (μm^2) at 12 weeks, respectively. There was no statistically significant difference in BIC values at any time point between control group and d-hMSCs group. ($p>0.05$)

As can be expected from the result of histologic analysis, New bone volume (BV%) measured within ROI in d-hMSCs group showed significantly increased new bone formation compared to that of control group. The average BV (%) values measured within ROI for control group (machined, SLA) were 7.47 % and 8.72 % at 2 weeks, and 19.27 % and 17.36 % at 12 weeks, respectively. The average BV (%) values measured within ROI for d-hMSCs group (machined, SLA) were 36.90 % and 49.64 % at 2 weeks, and 34.39 % and 53.07 % at 12 weeks, respectively. At 2 weeks, regardless of surface type, d-hMSCs group showed statistically significantly increased new bone formation compared to that of control group. ($p<0.05$) Although the average BV (%) values did not differ significantly between control group and d-hMSCs group with machined surface at

12 weeks, there was significant difference in BV (%) values between control group and d-hMSCs group with SLA surface.

When comparing the maturity of bone depending on the time point, Russell-Movat Pentachrome staining further confirmed that d-hMSCs group at 12 weeks showed higher histological maturity of bone than d-hMSCs group at 2 weeks. As shown in Figure 9, new bone network found in d-hMSCs group at 2 week stained as green/yellow, indicative of woven bone while new bone bridge found in d-hMSCs group at 12 week stained as red, indicative of lamellar bone and this color is similar to the intact bony tissue next to the defect. (Fig9)

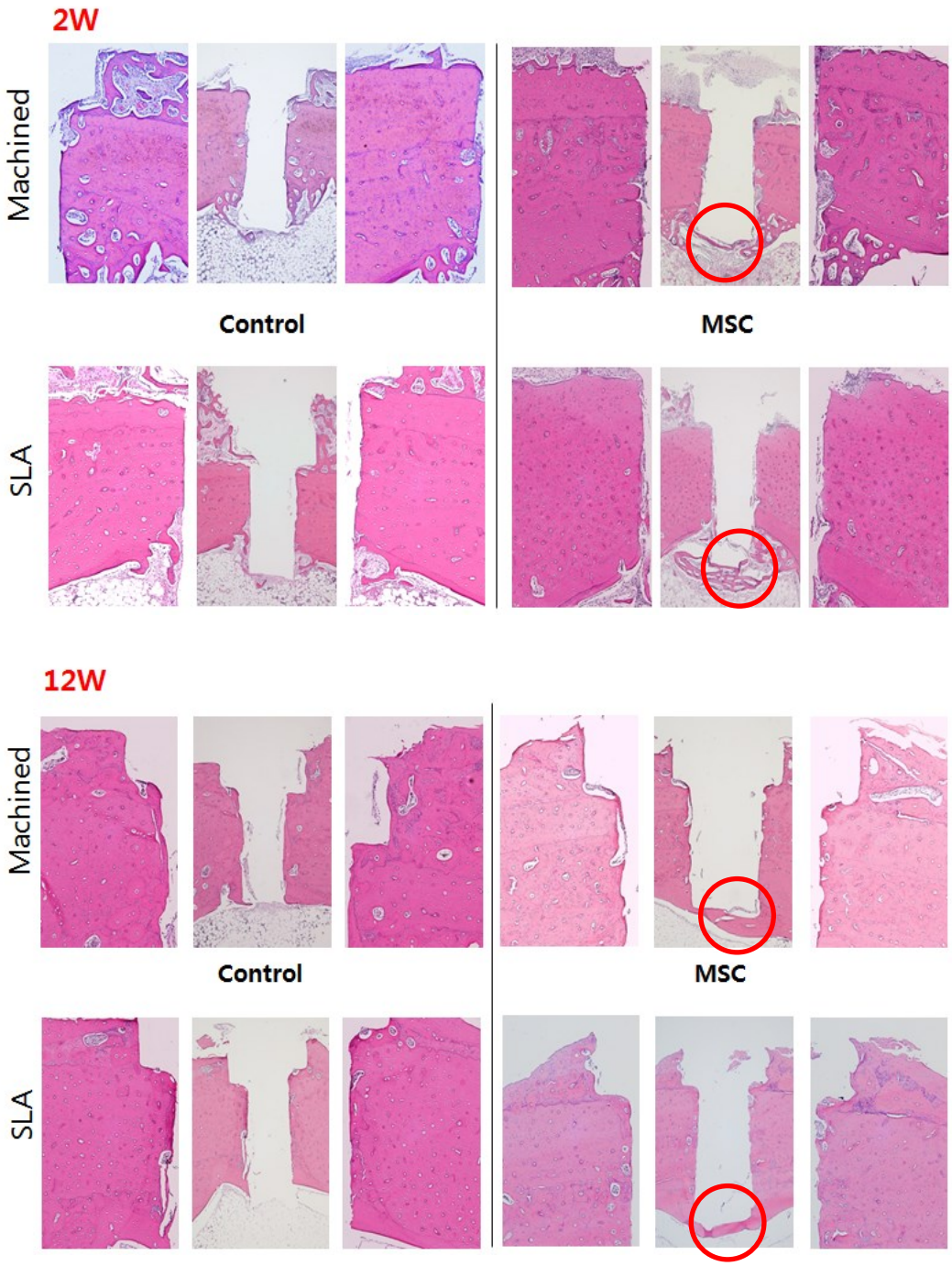

Fig7. Light-microscopy views of Control group (without d-hMSCs) and d-hMSCs groups sacrificed at 2 and 12 weeks postsurgery (Hematoxylin and eosin (H&E) stain, original magnification x50, x100)

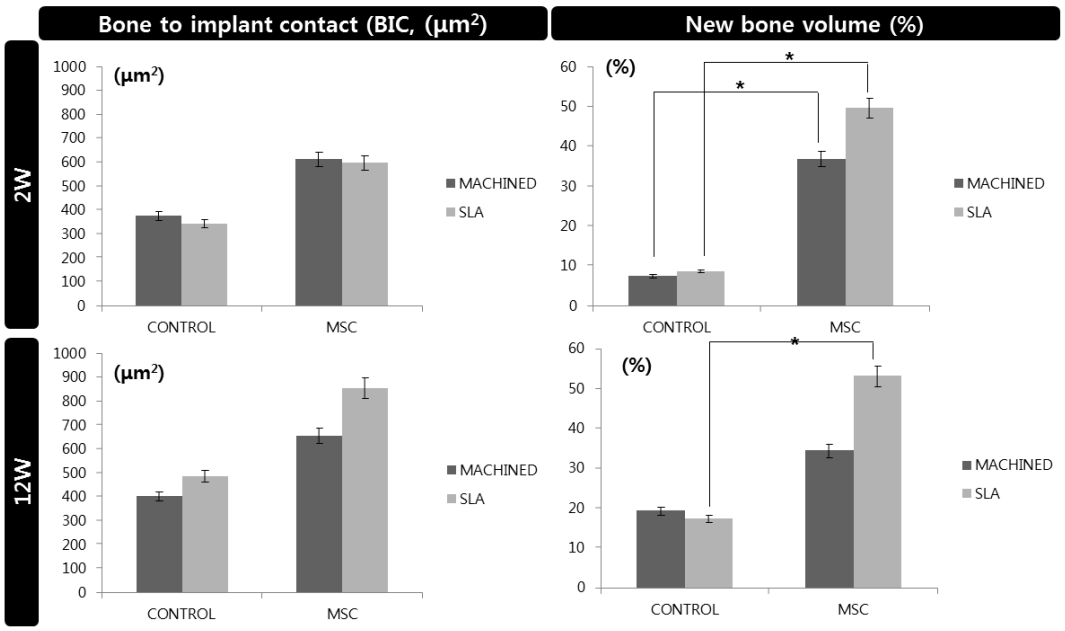

Fig8. Histomorphometric analysis Light-microscopy views of Control group (without d-hMSCs) and d-hMSCs groups sacrificed at 2 and 12 weeks postsurgery.

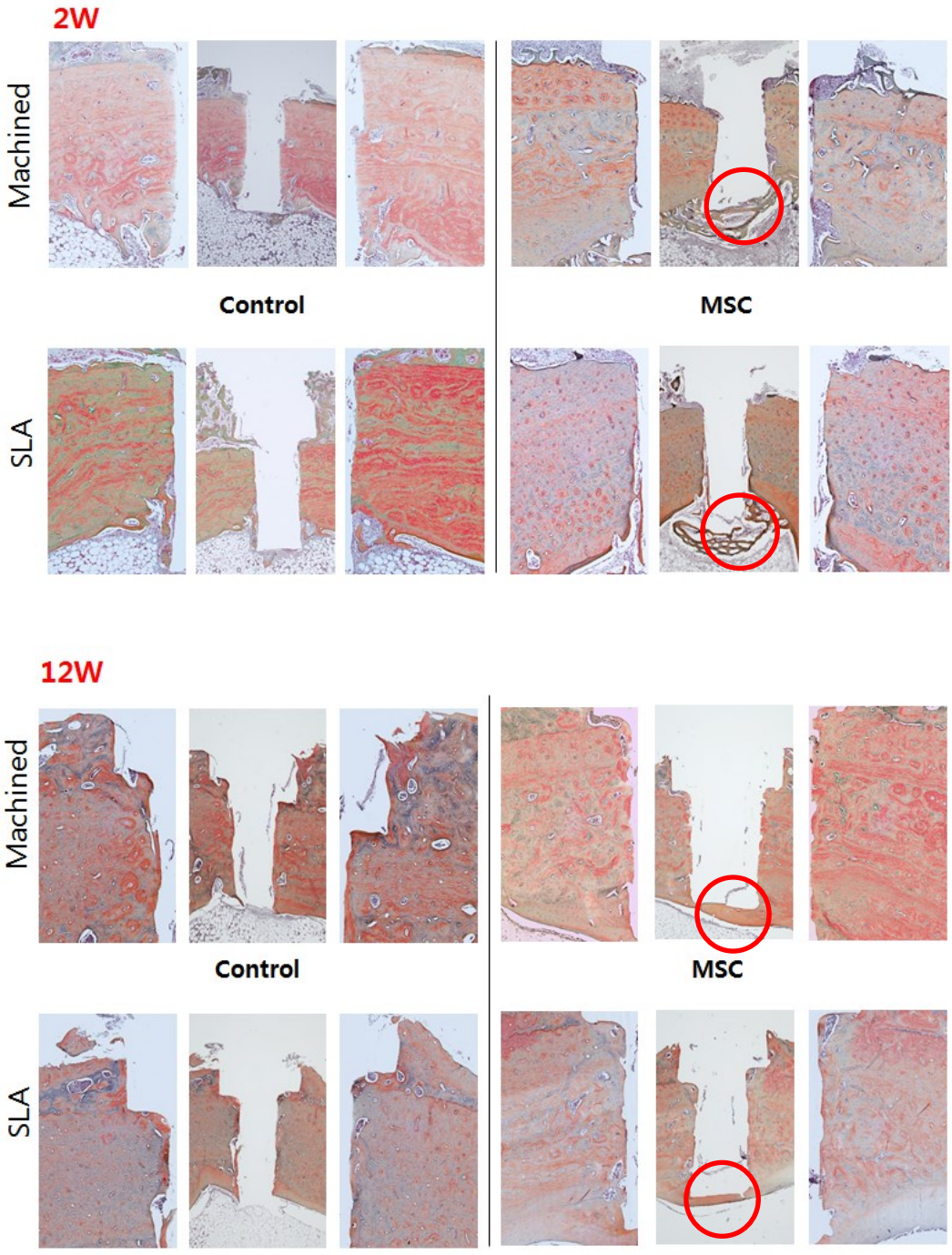

Fig9. Light-microscopy views of Control group (without d-hMSCs) and d-hMSCs groups sacrificed at 2 and 12 weeks postsurgery. (Russell-Movat pentachrome stain, original magnification x50, x100)

Immunohistochemistry

The immunohistochemical analysis revealed that Human Nuclei A exhibited to moderate to strong expression in d-hMSCs group at 2 week and the expression was mostly confined to the area below the implant, in which the d-hMSCs were most likely deposited. Partial expression was also identified alongside the body of implant. However, the level of expression was not as strong as that found in the bottom of the implant. At 12 weeks, Human Nuclei A still exhibited to week to moderate expression in d-hMSCs group, showing the survival of the d-hMSCs injected but the level of expression was weaker than that found at 2 week. (Fig10)

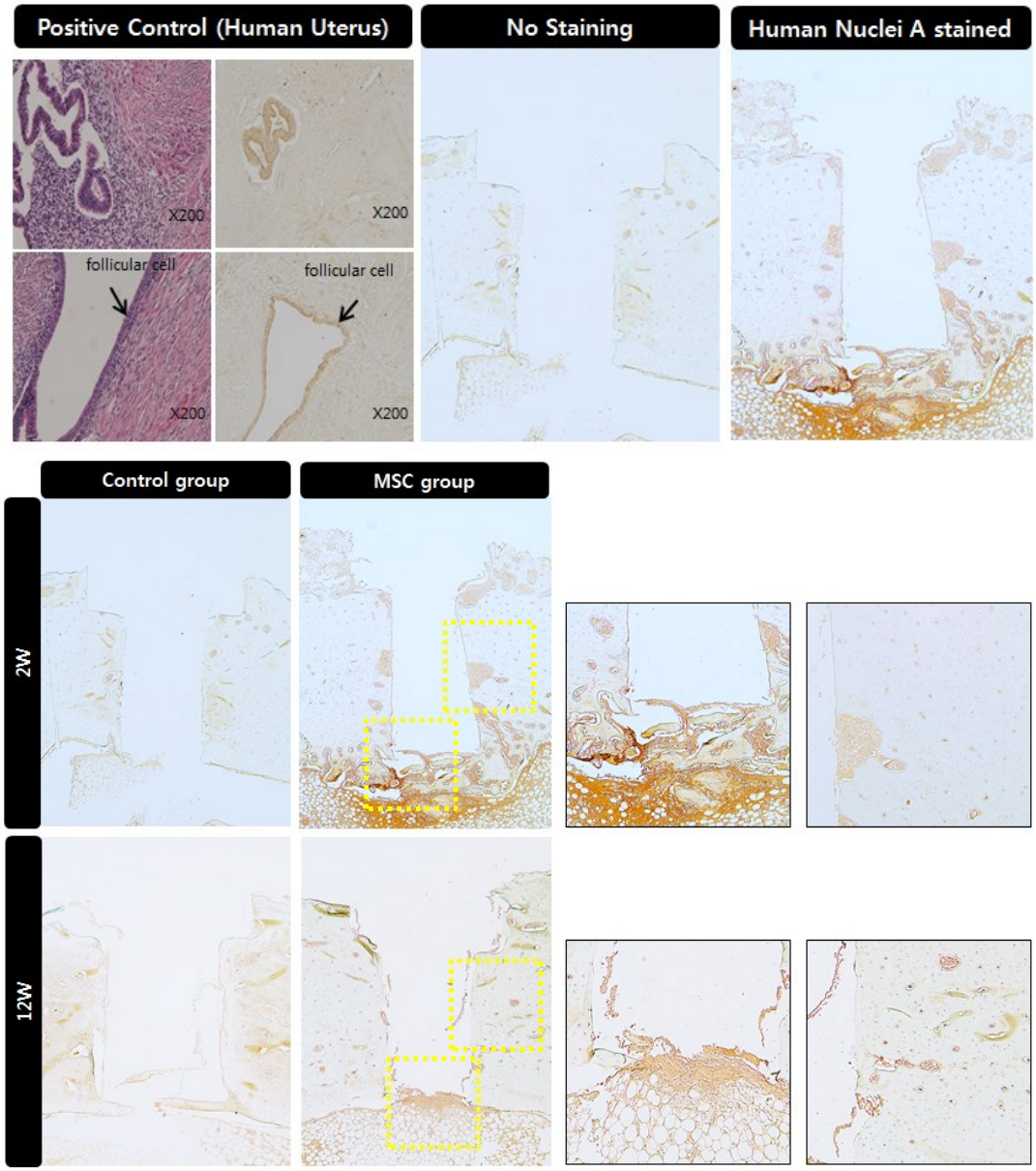

Fig10. Immunohistochemical analysis of Human nuclei A in Control group (without d-hMSCs) and d-hMSCs groups sacrificed at 2 and 12 weeks postsurgery.(original magnification x50, x100)

Ⅳ. DISCUSSION

Many contemporary literatures have demonstrated therapeutic benefits of engrafted hMSCs for local bone regeneration without any significant side effects. (50-53) However, several studies have also reported that most of engrafted hMSCs were not found in the target area and mostly died or entrapped in the lung if intravenously injected, limiting the use of hMSCs as a routine clinical application.(54) Indeed, more preclinical researches are required to accurately assess the therapeutic potential of hMSCs by mimicking site-specific clinical conditions. In this study, we attempted to investigate the behavior of d-hMSCs, which has more advantage than hMSCs obtained from bone marrow of iliac crest,(55, 56) in response to differently surface-treated implant, and also the effect of d-hMSCs on local osteogenesis around an implant depending on the different surface type has been evaluated using tibia model in rabbit.

The results from SEM analysis clearly showed that more active d-hMSCs cellular response was identified on SLA surface than machined surface and this difference became more disenable from day 5 of initial culture, showing circular nodule formation in a dispersed form. From day 7, mineralized crystalline-like structure was identifiable on SLA surface and on machined surface with osteogenic induction media while this feature could not be found with the cells cultured on machined surface without osteogenic induction media. These time-dependent, surface-dependent cellular morphological change were confirmed quantitatively throughout the result of RT-PCR, showing the

greater bone-related gene expression including COL-1, RUX2, IBSP and BGP on SLA surface although no statically significant difference in the level of expression was identified between SLA surface and machined surface.($p>0.05$) These results were in accordance with our previous study, which reported the increased early osteogenic markers (COL1, RUNX2) with dental stem cell derived induced pluripotent stem cell cultured on the SLA-treated titanium disc in comparison to machined titanium disc. (57) As reported in many previous studies,(26, 27, 58) it has been generally accepted that the rougher the implant surface, the more active hMSC cell response present in terms of adhesion to the surface and differentiation into osteoblast through activation of RhoA/ROCK pathway which ultimately influences the transcription factor RUNX2 to control osteoblast differentiation and matrix mineralization. (59, 60) Therefore, it was once more confirmed throughout this study that the cell response of d-hMSCs can be affected by the topography of implant materials and may be further anticipated that manipulating topography of implant surface could control the fate of d-hMSCs for bone tissue engineering applications.

In addition to the in vitro analysis of d-hMSCs, in vivo cell transplantation studies were also performed since the ultimate purpose of the present study was to evaluate if the d-hMSCs can survive on the defects and directly regenerate bone around an implant. Although calvarial defect models is a most frequently used defect model to assess in vivo osteogenesis, this model only evaluates intramembranous bone formation in a non-load bearing area. (61) Instead, we used tibia defect model in the present study to accurately access the bone-forming ability around implant placed in load bearing bone, which better

mimics actual clinical situation. Also, since it is well known that the choice of an appropriate scaffold, which should enables cell delivery, survival and attachment, is a pivotal factor in determining the success of cell transplantation, we used cytocompatible matrigel^{TM} which does not directly contribute to bone formation so that the pure osteogenic effect of cell transplantation can be deduced from the result of d-hMSCs group.

According to the result of radiographic and histomophometric analysis, the osteogenic effect d-hMSCs around implant was clearly identified, showing the greater new bone formation especially in early phase of bone regeneration. In addition to direct conversion of hMSC into osteoblast, Totelli et al. suggested 'indirect' action of hMSC, insisting engrafted hMSCs may act as 'signaling center', orchestrating the host response to the injury, especially in attracting host vasculature. (62) In the same point of view, Le Blanc K et al. reported that such 'trophic' or 'paracrine' effect of hMSCs can be critical in initial inflammatory phases as hMSCs are known to have anti-inflammatory functions. (63, 64) In this sense, the significant increase in bone formation in d-hMSCs group at 2 weeks can be interpreted in addition to their direct role as a source of new osteoblasts. These results are supported by the results of histomorphometric analysis in which significant difference in new bone volume (%) was identified solely in SLA surface group at 12 week whereas significant increased osteogenic effect of d-hMSC group was identified regardless of surface type. Again, it can be interpreted that the effect of d-hMSCs had been maximized in early phase of bone regeneration, followed by additional osteogenesis effect by SLA surface at later phase of bone regeneration.

Although it was not very hard to differentiate newly formed-bone quality between d-hMSCs group at 2 week and d-hMSCs group at 12 week from histologic images, the absolute value of new bone volume (%) did not show any difference. Therefore, Russell-Movat Pentachomre staining was employed in the present study to compare the maturity of bone depending on the time point and verified that d-hMSCs group at 12 weeks showed higher histological maturity of bone than d-hMSCs group at 2 weeks.

Lastly, but very importantly, we accesses the survival time of engrafted d-hMSCs, since it was reported that most of d-hMSCs are deemed to be dead or not function in target area which may result from various reasons including inappropriate cell density,(65) regulation of microenvironment(66) and high oxygen tension.(67) The immunohistochemical analysis revealed that Human Nuclei A still exhibited to week to moderate expression in in d-hMSCs group, showing the survival of the d-hMSCs up to 12 weeks posts engraftment although the level of expression was weaker than that found at 2 week, which suggests the attenuating of the function of d-hMSCs at 12 week.

In summary, all parameters investigated in this study including in vitro analysis, radiographic, histologic, histomorphometric, and immunohistochemical analysis were consistent with each other and reveled promising results that d-hMSCs enhances the new bone formation around an implant with the additional increase in osteogenic potential by SLA surface. Nevertheless, it has to be admitted that translations of these results into clinical practice may encounter many challenges beyond safety concerns described previously.(68) Further study may be required in attempt to improve the longevity of the

d-hMSCs and to determine the optimal conditions in which the osteogenic potency of d-hMSCs can be maximized.

Ⅴ. CONCLUSION

Collectively, within the limitation of the present study, transplantation of d-hMSCs along with use of appropriate implant surface type can be used as promising tools to reconstruct an appropriate regenerative microenvironment, thereby increasing bone regeneration capacity. This method may further provide a possible strategy for significantly reducing treatment time of current treatment modality incorporated with dental implant.

REFERENCES

1. Lange R, Luthen F, Beck U, Rychly J, Baumann A, Nebe B. Cell-extracellular matrix interaction and physico-chemical characteristics of titanium surfaces depend on the roughness of the material. Biomolecular engineering. 2002;19(2-6):255-61.
2. Anselme K. Osteoblast adhesion on biomaterials. Biomaterials. 2000;21(7):667-81.
3. Boyan BD, Lossdorfer S, Wang L, Zhao G, Lohmann CH, Cochran DL, et al. Osteoblasts generate an osteogenic microenvironment when grown on surfaces with rough microtopographies. European cells & materials. 2003;6:22-7.
4. Buser D, Dula K, Hess D, Hirt HP, Belser UC. Localized ridge augmentation with autografts and barrier membranes. Periodontology 2000. 1999;19:151-63.
5. Park KH, Koak JY, Kim SK, Heo SJ. Wettability and cellular response of UV light irradiated anodized titanium surface. The journal of advanced prosthodontics. 2011;3(2):63-8.
6. Prockop DJ. Marrow stromal cells as stem cells for nonhematopoietic tissues. Science. 1997;276(5309):71-4.
7. Dennis JE, Merriam A, Awadallah A, Yoo JU, Johnstone B, Caplan AI. A quadripotential mesenchymal progenitor cell isolated from the marrow of an adult mouse. Journal of bone and mineral research : the official journal of the American Society for Bone and Mineral Research. 1999;14(5):700-9.
8. Di Nicola M, Carlo-Stella C, Magni M, Milanesi M, Longoni PD, Matteucci P, et al. Human bone marrow stromal cells suppress T-lymphocyte proliferation induced by

cellular or nonspecific mitogenic stimuli. Blood. 2002;99(10):3838-43.

9. Krampera M, Glennie S, Dyson J, Scott D, Laylor R, Simpson E, et al. Bone marrow mesenchymal stem cells inhibit the response of naive and memory antigen-specific T cells to their cognate peptide. Blood. 2003;101(9):3722-9.
10. Petite H, Viateau V, Bensaid W, Meunier A, de Pollak C, Bourguignon M, et al. Tissue-engineered bone regeneration. Nature biotechnology. 2000;18(9):959-63.
11. Banerjee M, Bhonde RR. Autologous bone marrow transplantation/mobilization: a potential regenerative medicine for systemic degenerative disorders and healthy living. Medical hypotheses. 2007;68(6):1247-51.
12. Hynes K, Menicanin D, Han J, Marino V, Mrozik K, Gronthos S, et al. Mesenchymal stem cells from iPS cells facilitate periodontal regeneration. Journal of dental research. 2013;92(9):833-9.
13. Hayashi T, Misawa H, Nakahara H, Noguchi H, Yoshida A, Kobayashi N, et al. Transplantation of osteogenically differentiated mouse iPS cells for bone repair. Cell transplantation. 2012;21(2-3):591-600.
14. Okano H, Nakamura M, Yoshida K, Okada Y, Tsuji O, Nori S, et al. Steps toward safe cell therapy using induced pluripotent stem cells. Circulation research. 2013;112(3):523-33.
15. Hu K. All roads lead to induced pluripotent stem cells: the technologies of iPSC generation. Stem cells and development. 2014;23(12):1285-300.
16. Tong Z, Solanki A, Hamilos A, Levy O, Wen K, Yin X, et al. Application of biomaterials to advance induced pluripotent stem cell research and therapy. The

EMBO journal. 2015;34(8):987-1008.

17. Nomura Y, Ishikawa M, Yashiro Y, Sanggarnjanavanich S, Yamaguchi T, Arai C, et al. Human periodontal ligament fibroblasts are the optimal cell source for induced pluripotent stem cells. Histochemistry and cell biology. 2012;137(6):719-32.
18. Tamaoki N, Takahashi K, Tanaka T, Ichisaka T, Aoki H, Takeda-Kawaguchi T, et al. Dental pulp cells for induced pluripotent stem cell banking. Journal of dental research. 2010;89(8):773-8.
19. Wada N, Wang B, Lin NH, Laslett AL, Gronthos S, Bartold PM. Induced pluripotent stem cell lines derived from human gingival fibroblasts and periodontal ligament fibroblasts. Journal of periodontal research. 2011;46(4):438-47.
20. Ohnuki M, Takahashi K, Yamanaka S. Generation and characterization of human induced pluripotent stem cells. Current protocols in stem cell biology. 2009;Chapter 4:Unit 4A 2.
21. Park J, Bauer S, von der Mark K, Schmuki P. Nanosize and vitality: TiO2 nanotube diameter directs cell fate. Nano letters. 2007;7(6):1686-91.
22. Oh S, Brammer KS, Li YS, Teng D, Engler AJ, Chien S, et al. Stem cell fate dictated solely by altered nanotube dimension. Proceedings of the National Academy of Sciences of the United States of America. 2009;106(7):2130-5.
23. Takahashi K, Tanabe K, Ohnuki M, Narita M, Ichisaka T, Tomoda K, et al. Induction of pluripotent stem cells from adult human fibroblasts by defined factors. Cell. 2007;131(5):861-72.
24. Kim K, Doi A, Wen B, Ng K, Zhao R, Cahan P, et al. Epigenetic memory in induced

pluripotent stem cells. Nature. 2010;467(7313):285-90.

25. Wang CY, Zhao BH, Ai HJ, Wang YW. Comparison of biological characteristics of mesenchymal stem cells grown on two different titanium implant surfaces. Biomedical materials. 2008;3(1):015004.
26. Barone A, Toti P, Bertossi D, Marconcini S, De Santis D, Nocini PF, et al. Gene Expression of Human Mesenchymal Stem Cells Cultured on Titanium Dental Implant Surfaces. The Journal of craniofacial surgery. 2016;27(3):712-7.
27. Inzunza D, Covarrubias C, Von Marttens A, Leighton Y, Carvajal JC, Valenzuela F, et al. Synthesis of nanostructured porous silica coatings on titanium and their cell adhesive and osteogenic differentiation properties. Journal of biomedical materials research Part A. 2014;102(1):37-48.
28. Smith LA, Liu X, Hu J, Ma PX. The enhancement of human embryonic stem cell osteogenic differentiation with nano-fibrous scaffolding. Biomaterials. 2010;31(21):5526-35.
29. Khan MR, Donos N, Salih V, Brett PM. The enhanced modulation of key bone matrix components by modified Titanium implant surfaces. Bone. 2012;50(1):1-8.
30. Wall I, Donos N, Carlqvist K, Jones F, Brett P. Modified titanium surfaces promote accelerated osteogenic differentiation of mesenchymal stromal cells in vitro. Bone. 2009;45(1):17-26.
31. Olivares-Navarrete R, Hyzy SL, Hutton DL, Erdman CP, Wieland M, Boyan BD, et al. Direct and indirect effects of microstructured titanium substrates on the induction of mesenchymal stem cell differentiation towards the osteoblast lineage.

Biomaterials. 2010;31(10):2728-35.

32. Mante M, Daniels B, Golden E, Diefenderfer D, Reilly G, Leboy PS. Attachment of human marrow stromal cells to titanium surfaces. The Journal of oral implantology. 2003;29(2):66-72.
33. Logan N, Brett P. The Control of Mesenchymal Stromal Cell Osteogenic Differentiation through Modified Surfaces. Stem cells international. 2013;2013:361637.
34. Cochran DL, Nummikoski PV, Higginbottom FL, Hermann JS, Makins SR, Buser D. Evaluation of an endosseous titanium implant with a sandblasted and acid-etched surface in the canine mandible: radiographic results. Clinical oral implants research. 1996;7(3):240-52.
35. Eom TG, Jeon GR, Jeong CM, Kim YK, Kim SG, Cho IH, et al. Experimental study of bone response to hydroxyapatite coating implants: bone-implant contact and removal torque test. Oral surgery, oral medicine, oral pathology and oral radiology. 2012;114(4):411-8.
36. Duske K, Koban I, Kindel E, Schroder K, Nebe B, Holtfreter B, et al. Atmospheric plasma enhances wettability and cell spreading on dental implant metals. Journal of clinical periodontology. 2012;39(4):400-7.
37. Ogawa T. Ultraviolet photofunctionalization of titanium implants. The International journal of oral & maxillofacial implants. 2014;29(1):e95-102.
38. Kim MY, Choi H, Lee JH, Kim JH, Jung HS, Kim JH, et al. UV Photofunctionalization Effect on Bone Graft in Critical One-Wall Defect around

Implant: A Pilot Study in Beagle Dogs. BioMed research international. 2016;2016:4385279.

39. Klinker MW, Wei CH. Mesenchymal stem cells in the treatment of inflammatory and autoimmune diseases in experimental animal models. World journal of stem cells. 2015;7(3):556-67.
40. Pileggi A. Mesenchymal stem cells for the treatment of diabetes. Diabetes. 2012;61(6):1355-6.
41. Martin-Rendon E, Brunskill SJ, Hyde CJ, Stanworth SJ, Mathur A, Watt SM. Autologous bone marrow stem cells to treat acute myocardial infarction: a systematic review. European heart journal. 2008;29(15):1807-18.
42. Vainshtein JM, Kabarriti R, Mehta KJ, Roy-Chowdhury J, Guha C. Bone marrow-derived stromal cell therapy in cirrhosis: clinical evidence, cellular mechanisms, and implications for the treatment of hepatocellular carcinoma. International journal of radiation oncology, biology, physics. 2014;89(4):786-803.
43. Davies JE. Mechanisms of endosseous integration. The International journal of prosthodontics. 1998;11(5):391-401.
44. Davies JE. Understanding peri-implant endosseous healing. Journal of dental education. 2003;67(8):932-49.
45. Bigerelle M, Anselme K, Noel B, Ruderman I, Hardouin P, Iost A. Improvement in the morphology of Ti-based surfaces: a new process to increase in vitro human osteoblast response. Biomaterials. 2002;23(7):1563-77.
46. Yang Y, Tian J, Deng L, Ong JL. Morphological behavior of osteoblast-like cells on

surface-modified titanium in vitro. Biomaterials. 2002;23(5):1383-9.

47. Ku CH, Pioletti DP, Browne M, Gregson PJ. Effect of different Ti-6Al-4V surface treatments on osteoblasts behaviour. Biomaterials. 2002;23(6):1447-54.
48. Mayr-Wohlfart U, Fiedler J, Gunther KP, Puhl W, Kessler S. Proliferation and differentiation rates of a human osteoblast-like cell line (SaOS-2) in contact with different bone substitute materials. Journal of biomedical materials research. 2001;57(1):132-9.
49. Shi SR, Shi Y, Taylor CR. Antigen retrieval immunohistochemistry: review and future prospects in research and diagnosis over two decades. The journal of histochemistry and cytochemistry : official journal of the Histochemistry Society. 2011;59(1):13-32.
50. McAllister BS. Stem cell-containing allograft matrix enhances periodontal regeneration: case presentations. The International journal of periodontics & restorative dentistry. 2011;31(2):149-55.
51. McAllister BS, Haghighat K, Gonshor A. Histologic evaluation of a stem cell-based sinus-augmentation procedure. Journal of periodontology. 2009;80(4):679-86.
52. Park JB. Use of cell-based approaches in maxillary sinus augmentation procedures. The Journal of craniofacial surgery. 2010;21(2):557-60.
53. Razzouk S, Schoor R. Mesenchymal stem cells and their challenges for bone regeneration and osseointegration. Journal of periodontology. 2012;83(5):547-50.
54. Fischer UM, Harting MT, Jimenez F, Monzon-Posadas WO, Xue H, Savitz SI, et al. Pulmonary passage is a major obstacle for intravenous stem cell delivery: the

pulmonary first-pass effect. Stem cells and development. 2009;18(5):683-92.

55. Morad G, Kheiri L, Khojasteh A. Dental pulp stem cells for in vivo bone regeneration: a systematic review of literature. Archives of oral biology. 2013;58(12):1818-27.
56. Bright R, Hynes K, Gronthos S, Bartold PM. Periodontal ligament-derived cells for periodontal regeneration in animal models: a systematic review. Journal of periodontal research. 2015;50(2):160-72.
57. Choi H, Park KH, Lee AR, Mun CH, Shin YD, Park YB, et al. Control of dental-derived induced pluripotent stem cells through modified surfaces for dental application. Acta odontologica Scandinavica. 2017;75(5):309-18.
58. Olivares-Navarrete R, Hyzy SL, Park JH, Dunn GR, Haithcock DA, Wasilewski CE, et al. Mediation of osteogenic differentiation of human mesenchymal stem cells on titanium surfaces by a Wnt-integrin feedback loop. Biomaterials. 2011;32(27):6399-411.
59. Yao X, Peng R, Ding J. Effects of aspect ratios of stem cells on lineage commitments with and without induction media. Biomaterials. 2013;34(4):930-9.
60. Janson IA, Putnam AJ. Extracellular matrix elasticity and topography: material-based cues that affect cell function via conserved mechanisms. Journal of biomedical materials research Part A. 2015;103(3):1246-58.
61. Ko JY, Park S, Im GI. Osteogenesis from human induced pluripotent stem cells: an in vitro and in vivo comparison with mesenchymal stem cells. Stem cells and development. 2014;23(15):1788-97.

62. Tortelli F, Tasso R, Loiacono F, Cancedda R. The development of tissue-engineered bone of different origin through endochondral and intramembranous ossification following the implantation of mesenchymal stem cells and osteoblasts in a murine model. Biomaterials. 2010;31(2):242-9.
63. Le Blanc K, Pittenger M. Mesenchymal stem cells: progress toward promise. Cytotherapy. 2005;7(1):36-45.
64. Le Blanc K, Rasmusson I, Sundberg B, Gotherstrom C, Hassan M, Uzunel M, et al. Treatment of severe acute graft-versus-host disease with third party haploidentical mesenchymal stem cells. Lancet. 2004;363(9419):1439-41.
65. Sotiropoulou PA, Perez SA, Salagianni M, Baxevanis CN, Papamichail M. Characterization of the optimal culture conditions for clinical scale production of human mesenchymal stem cells. Stem cells. 2006;24(2):462-71.
66. Paschos NK, Brown WE, Eswaramoorthy R, Hu JC, Athanasiou KA. Advances in tissue engineering through stem cell-based co-culture. Journal of tissue engineering and regenerative medicine. 2015;9(5):488-503.
67. Carrancio S, Lopez-Holgado N, Sanchez-Guijo FM, Villaron E, Barbado V, Tabera S, et al. Optimization of mesenchymal stem cell expansion procedures by cell separation and culture conditions modification. Experimental hematology. 2008;36(8):1014-21.
68. Bieback K, Hecker A, Kocaomer A, Lannert H, Schallmoser K, Strunk D, et al. Human alternatives to fetal bovine serum for the expansion of mesenchymal stromal cells from bone marrow. Stem cells. 2009;27(9):2331-41.

국문요약

골 재생능 향상을 위한
치성줄기세포의 기능조절 및 적용연구

최현민

연세대학교 대학원 치의학과

(지도교수 박영범)

본 연구의 목적은 치성줄기세포 유래 만능유도 줄기세포(induced pluripotent stem cell derived from dental stem cells)를 제작, 배아줄기세포(embryonic stem cells)와 같은 특성을 가지고 있는지 확인하고 임플란트 표면 특성에 따라 치성줄기세포 유래 만능유도 줄기세포 및 치성줄기세포(dental stem cells)의 초기부착과 증식 및 분화에 미치는 영향을 분석하며 동물실험 모델에서 치성줄기세포의 주입이 골 형성능 향상에 미치는 영향을 방사선학적, 조직계측학적, 면역세포화학적으로 평가하는 것이다.

치주조직에서 치성 줄기세포주를 얻어 4 개의 야마나카 전사인자(OCT4, SOX2, cMyc, KLF4) 를 Sendai virus 에 삽입 후 배양, 약 7-10 일 후에 형질 변환된 유도 만능 줄기세포를 분리하고 세포 집합체를 이룰 때까지 약 7 일동안 추가적으로 배양하여 치성 줄기세포 유래 만능유도 줄기세포를 제작하였다. 만능 줄기세포 마커 확인, Alkaline Phosphatase 염색, Embryoid Body 형성 여부, 삼배엽 분화 여부, karyotyping 을 통해 특성 규명 연구를 시행하고 배아줄기세포와 같은 특성을 확인하였다. 지름 10mm 의 표면처리 되지 않은 원형 티타니움 디스크와 sandblasted, large-grit, acid-etched(SLA) 표면처리 된 티타니움 디스크 위에 제작된 유도만능 줄기세포를 분주하고 약 28 일 동안 세포의 부착, 증식 및 분화를 관찰, 정량적 및 정성적 분석을 실시하였다(SEM, in vitro osteogenesis assay, FACS analysis of osteogenic marker, RT-PCR). 분석결과 표면성질에 따라 세포의 부착양상 및 조골세포로의 분화도가 시간에 따라 달라짐을 확인할 수 있었으며 특히 rough surface 인 SLA 표면상에서 분화도가 유의 차 있게 증가함을 확인 할 수 있었다. ($p<0.05$)

총 20 마리의 New Zealand White rabbit tibia 부위에 지름 1.5mm 의 defect 형성 후 치성줄기세포-젤 복합체를 치성 줄기세포 미주입군(control)과 치성줄기세포 주입군 (experimental)에 따라 주입하고 미리 제작된 customized mini implant 를 표면 처리되지 않은 군과

SLA 표면처리된 군으로 나누어 2 주, 12 주 후에 시편을 채득하였다. SEM, RT-PCR 분석을 통해 in vitro 상에서 임플란트의 표면특성에 따라 치성줄기세포의 부착양상 및 분화도가 차이가 있음을 확인하고 채득한 샘플에 대해 방사선학적, 조직계측학적, 면역세포화학적 분석을 실시 하였다. 분석 결과 치성줄기세포의 골 재생능 향상효과가 식립 된 부위의 위치의 골질에 따라, 희생시기에 따라 다르게 나타남을 확인 할 수 있었으며 임플란트의 표면처리 여부와 관계없이 치성줄기세포 주입 군에서 향상된 골 재생능을 확인 할 수 있었다.

본 연구의 제한점 안에서 임플란트 표면 특성에 따라 치성줄기세포 및 치성줄기세포 유래 만능유도 줄기세포의 기능을 조절 할 수 있고 치성줄기세포의 주입이 골 재생능 향상에 효과가 있다는 것을 확인 할 수 있었다. 따라서 임플란트 및 임플란트 관련 질환에서 치성줄기세포를 이용한 맞춤형 세포치료의 임상적용 가능성을 확인하고 향후 불량한 골질에서 신생골 형성능을 향상 시킬 수 있는 하나의 치료방법으로 제시 될 수 있을 것이라 사료된다.

핵심 되는 말 : 치성 줄기세포유래 만능유도 줄기세포, 치성줄기세포, 임플란트 표면, 골 재생, 세포치료, 토끼